JOC The Journal of Organic Chemistry

pubs.acs.org/joc Article

Mechanistic Insights into the $FeCl_3$-Catalyzed Oxidative Cross-Coupling of Phenols with 2-Aminonaphthalenes

Vlada Vershinin,[‡] Hagit Forkosh,[‡] Mor Ben-Lulu, Anna Libman, and Doron Pappo*

Cite This: *J. Org. Chem.* 2021, 86, 79–90 Read Online

ACCESS | Metrics & More | Article Recommendations | Supporting Information

ABSTRACT: The selective $FeCl_3$-catalyzed oxidative cross-coupling reaction between phenols and primary, secondary, and tertiary 2-aminonaphthalene derivatives was investigated. The generality of this scalable method provides a sustainable alternative for preparing *N,O*-biaryl compounds that are widely used as ligands and catalysts. Based on a comprehensive kinetic investigation, a catalytic cycle involving a ternary complex that binds to both the coupling partners and the oxidant during the key oxidative coupling step is postulated. Furthermore, the studies showed that the reaction is regulated by off-cycle acid–base and ligand exchange processes.

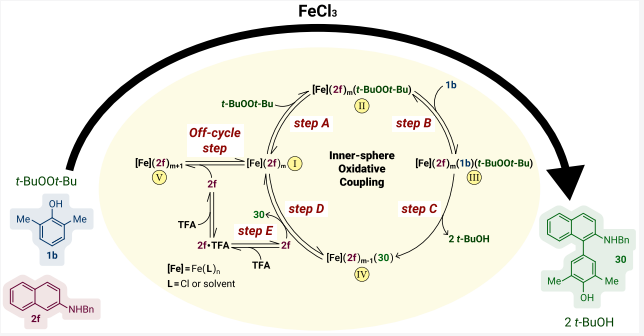

INTRODUCTION

Iron-catalyzed oxidative phenol coupling reactions[1] bring together phenols with unfunctionalized C–H nucleophiles such as 1,3-dicarbonyl compounds,[2] conjugated alkenes,[3] arenes, polyaromatic hydrocarbons (PAHs),[2b,4] and a second phenolic coupling partner.[5] This method is considered to be highly attractive in terms of step- and atom-economy for assembling new phenolic architectures.[6] As part of our group research program, we aimed to extend this reaction for the coupling of anilines to afford *N,O*-biaryl compounds that are widely used in asymmetric transformations.[7] Anilines and phenols share some of the same properties: they are both electron-rich cyclic π-systems that are prone to oxidation, generating a highly reactive electrophilic radical species.[8] Therefore, the development of selective oxidative cross-coupling reactions between phenols and unprotected anilines is a challenging task that has rarely been achieved.[9]

In an early work, Kočovský studied the reaction between 2-naphthol **1a** and 2-aminonaphthalene **2a** using a stoichiometric amount of a redox copper amine complex,[9k,l,n] affording (±)-2-amino-2′-hydroxy-1,1′-binaphthyl **3** (NOBIN, Scheme 1A). Recently, the Shindo group has developed aerobic oxidative cross-coupling conditions based on a heterogeneous Rh/C catalyst for the reaction between tertiary *N,N*-dialkylamino-2-naphthalenes and different nucleophiles, such as *N,N*-dialkylanilines, arenes, and phenols (Scheme 1A).[9f,10] Lately, our group has developed an M[TPP]Cl (M = Fe or Mn, TPP = 5,10,15,20-tetraphenyl-21H,23H-porphine)-catalyzed *para*-selective oxidative amination of phenols by primary and secondary anilines (Scheme 1B).[11] We have demonstrated that, depending on the identity of the phenolic *para*-R group, the products of this coupling are either benzoquinone anils (when R = H or OMe) or *N,O*-biaryl compounds (when R = alkyl). In a previous paper, we developed a two-step synthesis of optically pure NOBIN derivatives. The practical method is based on a stereoselective $FeCl_3$-catalyzed oxidative cross-coupling between 2-naphthols (e.g., **1a**, 1.5 equiv) and 2-aminonaphthalenes with a labile chiral auxiliary group (such as **2c**, 1 equiv, Scheme 1C),[12] affording a mixture of two separable NOBIN diastereoisomers [e.g., (R_a,*S*)-**5** and (S_a,*S*)-**5**]. A simple hydrogenolysis of the auxiliary group (H_2, Pd/C) offers a direct entry to the desirable (R_a)-**3** and (S_a)-**3** NOBINs in excellent chemical yields. Intrigued by the high degree of cross-coupling selectivity and the excellent yields imparted by the $FeCl_3$/TFA/*t*-BuOO*t*-Bu catalytic system, we were interested in probing the underlying mechanism and studying the generality of this method for the preparation of *N,O*-biaryl compounds (Scheme 1D).

The general mechanistic line for the oxidative coupling of phenols by iron catalysts involves three key steps: (1) the formation of high-valent iron-phenolate complexes, (2) the generation of a ligated phenoxyl radical intermediate, and (3) coupling with a π-nucleophile or a radical species.[1a] Recent mechanistic studies by our group for the $FeCl_3$-catalyzed oxidative homo- and cross-coupling reaction of phenols revealed a zero-order dependence on the [phenol].[5b] Based on these results, it was suggested that a multicoordinated iron

Received: April 9, 2020
Published: December 9, 2020

https://dx.doi.org/10.1021/acs.joc.0c00874
J. Org. Chem. 2021, 86, 79–90

Scheme 1. (A) Oxidative Cross-Coupling between 2-Naphthols and 2-Aminonaphthalene Derivatives, (B) the M[TPP]Cl-Catalyzed Oxidative Amination of Phenols by Anilines, (C) the Stereoselective Synthesis of NOBINs, and (D) Mechanistic and Scope Studies of the $FeCl_3$-Catalyzed Oxidative Phenol-2-Aminonaphthalene Coupling (This Work)

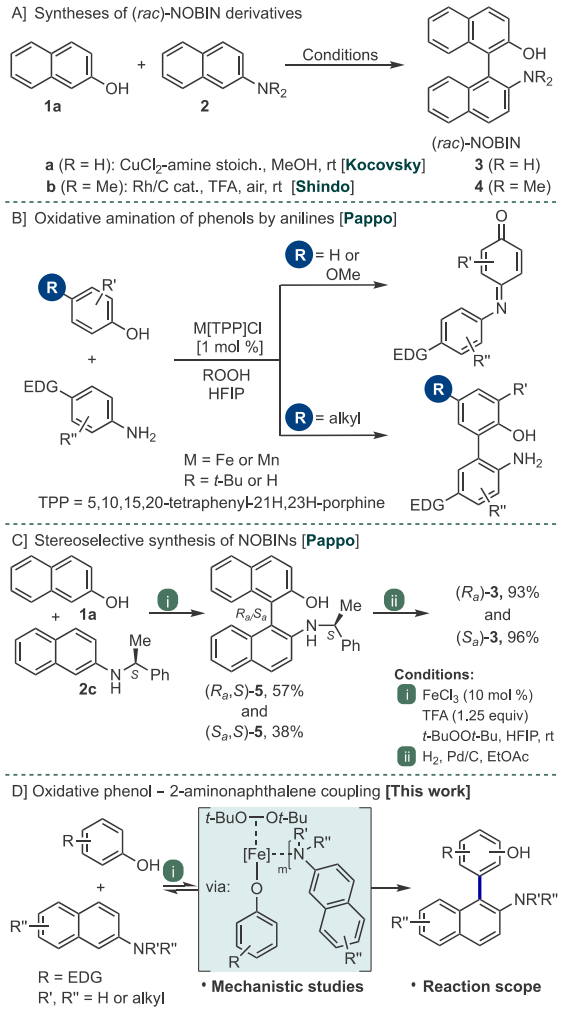

catalyst mediates an inner-sphere oxidative radical−anion coupling between two neighboring ligands (Figure 1A).[5b] However, the partial order for the phenolic component is no longer zero when the catalyst has a limited number of vacant sites, as exemplified by Katsuki [(Fe[μ-OH][salen])$_2$ catalyst][13] and Pappo [Fe[phosphate]$_3$ catalyst] (Figure 1B).[5c]

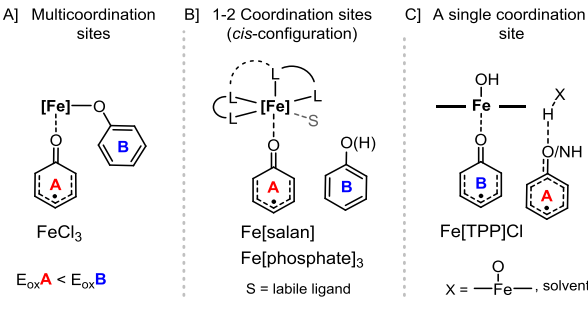

Figure 1. Relationship between the coupling mechanisms and the catalyst structure.

Furthermore, when the reaction is mediated by Fe[TPP]Cl, which has only a single axial position available for binding, the coupling takes place between a ligated phenoxyl radical and a liberated phenoxyl[5a] or an anilino radical[11] by an outer-sphere radical−radical coupling mechanism (Figure 1C). These studies show that the coupling mechanism changes as a function of the iron coordination sphere. Therefore, the selectivity and the efficiency of the oxidative coupling are expected to be affected by the relative binding strengths of the two coupling partners to the redox iron complex.

Herein, we report that $FeCl_3$ is an efficient catalyst for the oxidative coupling between readily oxidized phenols and primary, secondary, and tertiary 2-aminonaphthalene derivatives. The selective conditions were successfully applied for the synthesis of a long list of novel *N*,*O*-biaryl compounds that are needed as ligands in catalysis. Our comprehensive mechanistic studies support the existence of an inner-sphere coupling mechanism between a phenoxyl radical and a 2-aminonaphthalene ligand. Furthermore, initial rate kinetic experiments uncovered (a) the involvement of a ternary complex that binds to both the coupling partners and the oxidant during the key oxidative coupling step and (b) the existence of two off-cycle acid−base and ligand exchange processes that regulate the reaction rate.

RESULTS AND DISCUSSION

Method Development and Reaction Scope. Our research commenced by applying oxidative phenol−phenol coupling conditions [$FeCl_3$ (10 mol %), *t*-BuOO*t*-Bu (1.5 equiv), HFIP, and room temperature], which were developed by our group,[1a,4,5b,14] for reacting 2-naphthol **1a** (1.5 equiv) with 2-aminonaphthalene **2a** (1 equiv). Fortunately, this reaction proceeded smoothly, affording (*rac*)-NOBIN **3** in 82% yield (Figure 2). However, when secondary and tertiary 2-aminonaphthalene derivatives, *N*-butyl-2-aminonaphthalene **2d** and piperidino-2-naphthalene **2e**, respectively, were reacted with 2-naphthol **1a**, poor conversions were observed. Our study revealed that the addition of TFA (1.25 equiv) to the reaction between **1a** and the secondary 2-aminonaphthalene **2d** significantly improved the reaction efficiency, affording NOBIN **6** in 79% yield (Figure 2).[12] However, with piperidino-2-naphthalene **2e**, a higher concentration of TFA (3.75 equiv) was needed to ensure efficient and highly selective coupling, affording NOBIN **7** in 97% yield (Figure 2).

The scope of the reaction was further explored by reacting various 3- or 6-substituted-2-naphthols with 3-, 6-, and/or *N*-substituted-2-aminonaphthalene derivatives (Figure 2). Under the general conditions (*rac*)-NOBINs **3**, **6**−**17** were prepared in moderate to excellent yields (60−97%). An oxidative coupling between substituted phenols and *N*-substituted-2-aminonaphthalene derivatives is also possible, affording *N*,*O*-biaryl compounds **18**−**30** with high chemoselectivity and with yields that varied between 38 and 98% (Figure 3). Importantly, oxidizable functional groups, such as *para*-methoxybenzyl (compounds **9**, **10**, **14**, **23**, and **25**) and conjugate alkenes (**13** and **28**), survived the mild oxidation conditions. Finally, the scalability of the process was demonstrated by preparing compound **30** on a 2 mmol scale, and the structure of compound **20** was confirmed by X-ray diffraction analysis.

Mechanistic Studies. With the aim to elucidate a detailed catalytic cycle that will rationalize the observed reactivity and selectivity, a set of kinetic experiments were performed. The oxidative cross-coupling between 2,6-dimethylphenol (**1b**) and

https://dx.doi.org/10.1021/acs.joc.0c00874
J. Org. Chem. 2021, 86, 79−90

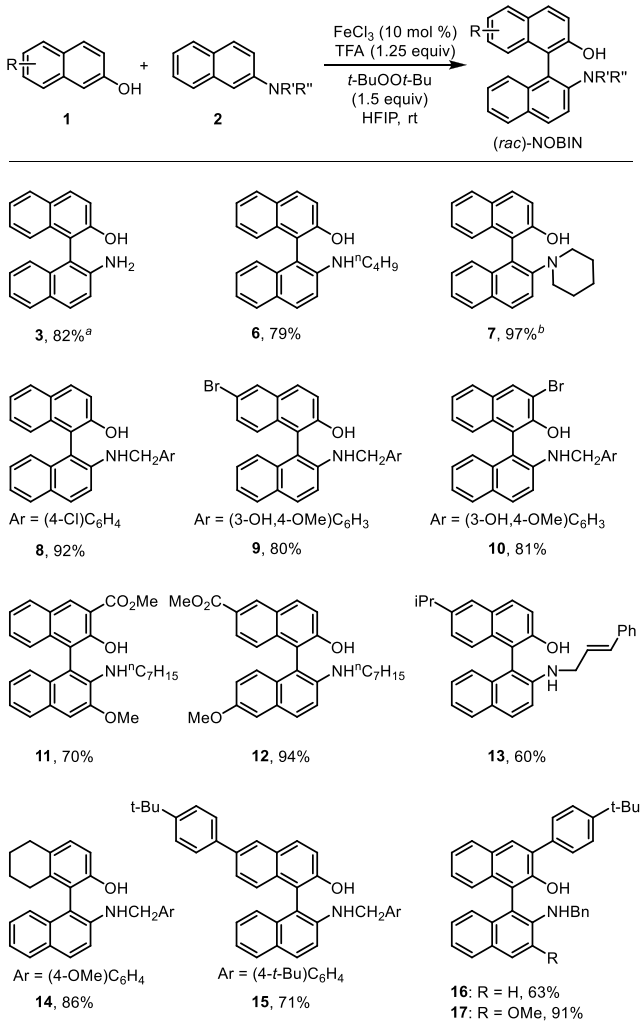

Figure 2. Scope of the oxidative coupling between 2-naphthols and 2-aminonaphthalene derivatives. Reaction conditions: 2-naphthol (1.5 equiv), 2-aminonaphthalene (1 equiv), $FeCl_3$ (10 mol %), *t*-BuOO*t*-Bu (1.5 equiv), TFA (1.25 equiv), HFIP (0.5 M), room temperature, and 24 h. [a]The reaction was performed without TFA. [b]The reaction was performed with 3 equiv of 2-naphthol **1a**, 4.5 equiv of *t*-BuOO*t*-Bu, and 3.75 equiv of TFA in total.

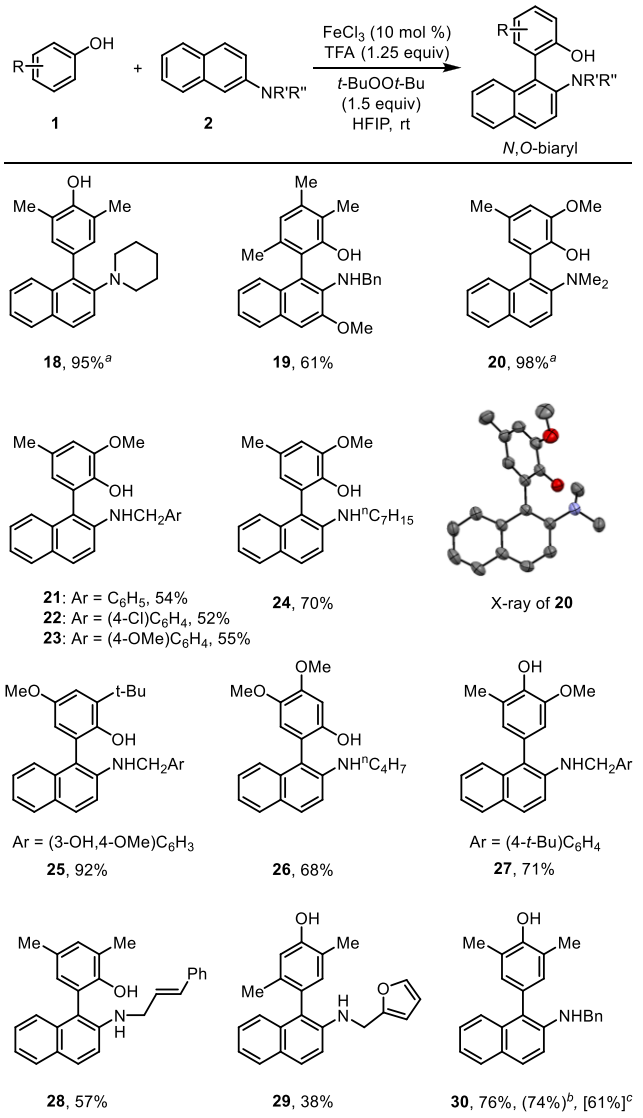

Figure 3. Scope of the oxidative coupling between substituted phenols and 2-aminonaphthalene derivatives. Reaction conditions: phenol (1.5 equiv), 2-aminonaphthalene (1 equiv), $FeCl_3$ (10 mol %), *t*-BuOO*t*-Bu (1.5 equiv), TFA (1.25 equiv), HFIP (0.5 M), room temperature, and 24 h. [a]The reaction was performed with 3 equiv of *t*-BuOO*t*-Bu and 2.5 equiv of TFA in total. [b]The reaction was performed on a 2 mmol scale. [c]The conditions were similar, except for phenol (1 equiv).

N-benzyl-2-aminonaphthalene (**2f**) was chosen since this transformation showed a high degree of cross-coupling selectivity.[15] First, the dependence of [phenol **1b**], [*t*-BuOO*t*-Bu], and [$FeCl_3$] on the reaction rate was investigated. The results show (i) a saturation curve for phenol **1b**, first order at a low concentrations range (0.02−0.1 M; see Figure 4A and Figure S1 in the Supporting Information) and close to a zero-order dependency at a high concentrations range (0.1−0.3 M); (ii) a positive rate dependence for *t*-BuOO*t*-Bu is found when the experiment was performed at a high level of [**1b**] (0.25 M, Figure 5A); and (iii) first order in the catalyst was observed for $FeCl_3$ (Figure 6A).

The reaction does not take place in the absence of the redox catalyst, as confirmed by the zero intercept and our control experiments. The existence of free radical mechanisms was ruled out since the addition of butylated hydroxytoluene (BHT) to the reaction mixture had no effect on the coupling yield (see the Supporting Information). Furthermore, these kinetic results strengthen the premise that *t*-BuOO*t*-Bu binds to the iron catalyst prior to the slow oxidative coupling step,[2a,5c] ruling out its action as a terminal oxidant that regenerates Fe(III) from Fe(II) after the coupling step.

The initial rate kinetic study indicated that **1b**, *t*-BuOO*t*-Bu, and **2f**, which showed negative order dependency (vide infra), are bound to the iron prior to the irreversible oxidative coupling step. Therefore, a kinetic behavior that characterizes a ternary enzyme (E, Figure 7) was considered. The action of ternary enzymes has been comprehensively studied by Cleland[15] and others.[16] These studies indicate that the mechanistic scheme of Bi-substrate enzyme-catalyzed reactions is characterized by a reversible binding of two substrates (**A** and **B**) to the enzyme prior to the slow step (E·**A**·**B** → products). The formation of E·**A**·**B** by the sequential binding of **A** and **B** can take place either via "random" or "ordered" sequential mechanisms. In a random mechanism, E·**A**·**B** is obtained from both E·**A** and E·**B**; i.e., the dissociation

https://dx.doi.org/10.1021/acs.joc.0c00874
J. Org. Chem. 2021, 86, 79−90

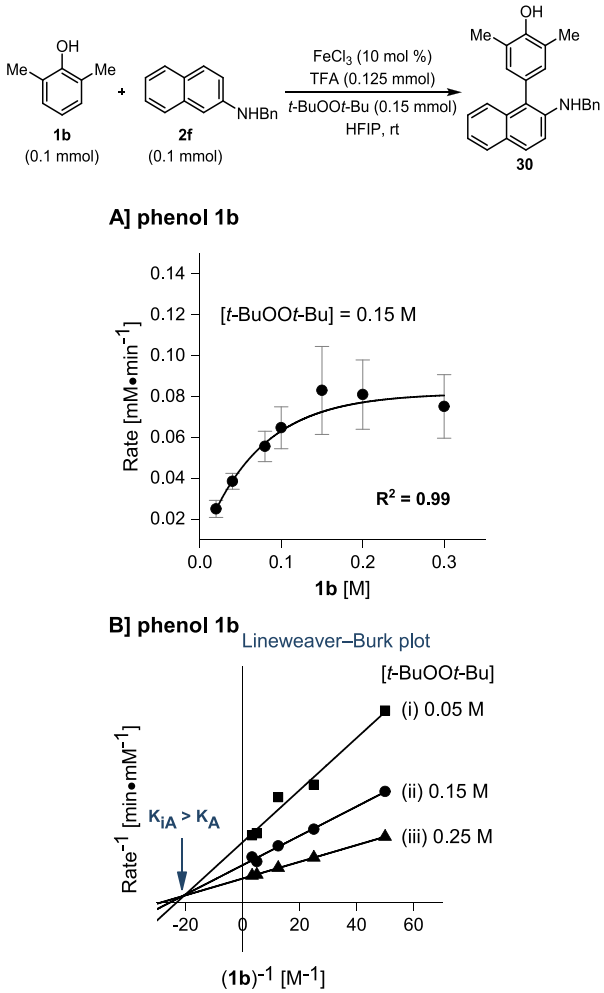

Figure 4. Initial rate kinetic studies for phenol **1b**. (A) Conditions: phenol **1b** (0.02, 0.04, 0.08, 0.1, 0.15, 0.2, and 0.3 mmol), 2-aminonaphthalene **2f** (0.1 mmol), TFA (0.125 mmol), $FeCl_3$ (0.01 mmol), *t*-BuOO*t*-Bu (0.15 mmol), and HFIP (1 mL). (B) Conditions: (i) phenol **1b** (0.02, 0.04, 0.08, 0.2, and 0.3 mmol), 2-aminonaphthalene **2f** (0.1 mmol), TFA (0.125 mmol), $FeCl_3$ (0.01 mmol), *t*-BuOO*t*-Bu (0.05 mmol), and HFIP (1 mL); (ii) phenol **1b** (0.02, 0.04, 0.08, 0.2, and 0.3 mmol), 2-aminonaphthalene **2f** (0.1 mmol), TFA (0.125 mmol), $FeCl_3$ (0.01 mmol), *t*-BuOO*t*-Bu (0.15 mmol), and HFIP (1 mL); (iii) phenol **1b** (0.02, 0.04, 0.08, 0.2, and 0.3 mmol), 2-aminonaphthalene **2f** (0.1 mmol), TFA (0.125 mmol), $FeCl_3$ (0.01 mmol), *t*-BuOO*t*-Bu (0.25 mmol), and HFIP (1 mL). The rates of the formation of product **30** in the initial stage of the reaction were determined by HPLC, using mesitylene as the initial standard.

constants of substrates to the free enzyme (K_{iA} for **A** and K_{iB} for **B**) and from E·**A**·**B** to enzymes E·**A** and E·**B** (K_A and K_B, respectively) are equal ($K_{iA} = K_A$ and $K_{iB} = K_B$).[17] However, in an ordered sequential mechanism E·**A**·**B** is obtained solely from E·**A** if substrate **A** binds preferentially to the free enzyme E ($K_{iA} < K_A$ and $K_{iB} > K_B$) or solely from E·**B** if binding of substrate **A** to this complex occurs in higher affinity ($K_{iA} > K_A$ and $K_{iB} < K_B$).[18]

The order in which phenol **1b** and *t*-BuOO*t*-Bu bind to the iron catalyst (assuming that E = [Fe](**2f**)$_m$] was determined by performing a set of double-reciprocal analysis experiments.[19] First, phenol **1b** (assigned as substrate **A**) was varied at fixed concentrations of *t*-BuOO*t*-Bu (0.05, 0.15, and 0.25 M, Figure 4B; see also Figure S1 in the Supporting Information) and then

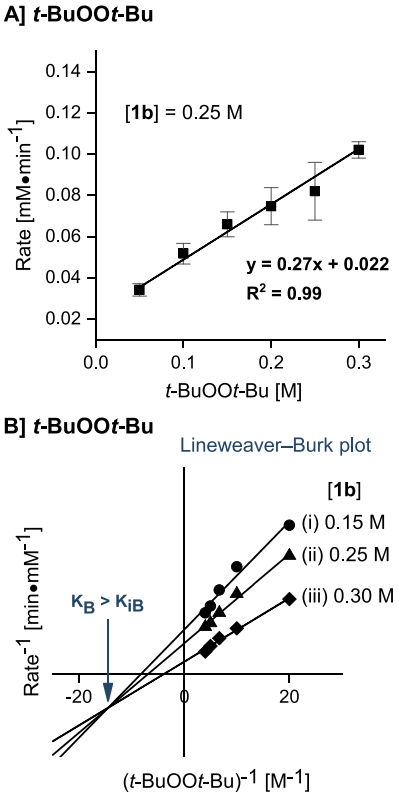

Figure 5. Initial rate kinetic studies for *t*-BuOO*t*-Bu. (A) Conditions: *t*-BuOO*t*-Bu (0.05, 0.1, 0.15, 0.2, 0.25, and 0.3 mmol), phenol **1b** (0.25 mmol), 2-aminonaphthalene **2f** (0.1 mmol), TFA (0.125 mmol), $FeCl_3$ (0.01 mmol), and HFIP (1 mL). (B) Conditions: (i) *t*-BuOO*t*-Bu (0.05, 0.1, 0.15, 0.2, and 0.25 mmol), phenol **1b** (0.15 mmol), 2-aminonaphthalene **2f** (0.1 mmol), TFA (0.125 mmol), $FeCl_3$ (0.01 mmol), and HFIP (1 mL); (ii) *t*-BuOO*t*-Bu (0.05, 0.1, 0.15, 0.2, and 0.25 mmol), phenol **1b** (0.25 mmol), 2-aminonaphthalene **2f** (0.1 mmol), TFA (0.125 mmol), $FeCl_3$ (0.01 mmol), and HFIP (1 mL); (iii) *t*-BuOO*t*-Bu (0.05, 0.1, 0.15, 0.2, and 0.25 mmol), phenol **1b** (0.30 mmol), 2-aminonaphthalene **2f** (0.1 mmol), TFA (0.125 mmol), $FeCl_3$ (0.01 mmol), and HFIP (1 mL). The rates of the formation of product **30** in the initial stage of the reaction were determined by HPLC, using mesitylene as the internal standard.

t-BuOO*t*-Bu (assigned as substrate **B**) was varied at fixed [phenol **1b**] values (0.15, 0.25, and 0.30 M, Figure 5B; see also Figure S2 in the Supporting Information). The Lineweaver–Burk plot for the phenol (Figure 4B) shows linear lines that intersect above the horizontal axis, whereas the position of the crossover point for the peroxide's linear lines (Figure 5B) is below the *x*-axis. According to Frieden analysis,[19] these results indicate that $K_{iA} > K_A$ and $K_{iB} < K_B$ (Figure 7, Eq. 3),[16,17,19,20] suggesting that [Fe]·(**2f**)$_m$·(**1b**)·(*t*-BuOO*t*-Bu) **III** is formed from [Fe]·(**2f**)$_m$ **I** by a sequential binding of the peroxide (step A, Scheme 2) and the phenol (Step B).

The dependence of 2-aminonaphthalene **2f** on the reaction velocity was examined (Figure 6B). The negative relationship between the reaction rate and [**2f**] indicates the presence of a competitive off-cycle equilibrium.[21] It is suggested that the association of the peroxide and the phenol to complex **I** (step A, Scheme 2) is suppressed by the competitive binding of **2f**, affording [Fe]·(**2f**)$_{m+1}$ (**V**, off-cycle step, Scheme 2). Consequently, the rate of the coupling decelerates as [**2f**] increases. These results also support the assumption that 2-

https://dx.doi.org/10.1021/acs.joc.0c00874
J. Org. Chem. 2021, 86, 79−90

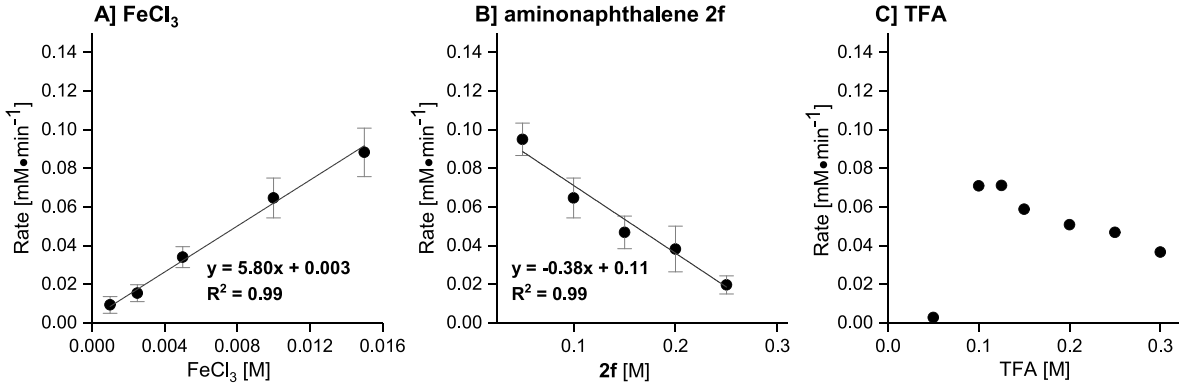

Figure 6. Initial rate kinetic studies for (A) conditions: $FeCl_3$ (0.001, 0.0025, 0.005, 0.01, and 0.015 mmol), phenol **1b** (0.1 mmol), 2-aminonaphthalene **2f** (0.1 mmol), TFA (0.125 mmol), *t*-BuOO*t*-Bu (0.15 mmol), and HFIP (1 mL). (B) Conditions: 2-aminonaphthalene **2f** (0.05, 0.1, 0.15, 0.2, and 0.25 mmol), phenol **1b** (0.1 mmol), TFA (1.25 equiv according to the concentration of **2f**), $FeCl_3$ (0.01 mmol), *t*-BuOO*t*-Bu (0.15 mmol), and HFIP (1 mL). (C) Conditions: TFA (0.05, 0.1, 0.125, 0.15, 0.2, 0.25, and 0.3 mmol), phenol **1b** (0.1 mmol), 2-aminonaphthalene **2f** (0.1 mmol), $FeCl_3$ (0.01 mmol), *t*-BuOO*t*-Bu (0.15 mmol), and HFIP (1 mL). The rates of the formation of product **30** in the initial stage of the reaction were determined by HPLC, using mesitylene as the internal standard.

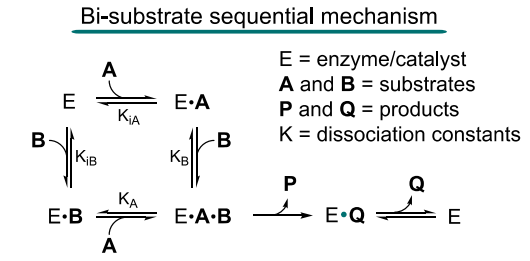

The general rate equation for a bi-substrate sequential mechanism:

Eq.1

$$v = \frac{V_{max}[A][B]}{K_{iA}K_B + K_A[B] + K_B[A] + [A][B]}$$

The general rate equation in a double reciprocal form:

Eq.2

$$\frac{1}{v} = rate^{-1} = \left[\frac{K_A}{V_{max}}\left(1 + \frac{K_{iA}K_B}{K_A[B]}\right)\right]\frac{1}{[A]} + \frac{1}{V_{max}}\left(1 + \frac{K_B}{[B]}\right)$$

At the crossover point, the same $\frac{1}{v}$ value is obtained for different [**B**], therefore

Eq.3

$$\frac{1}{v} = \frac{1}{V_{max}}\left(1 - \frac{K_A}{K_{iA}}\right)$$

$K_A = K_{iA}$ then the lines intersect on X-axis
$K_{iA} > K_A$ then the lines intersect above X-axis
$K_{iA} < K_A$ then the lines intersect below X-axis

In a similar manner for different [**A**]:

$$\frac{1}{v} = \frac{1}{V_{max}}\left(1 - \frac{K_B}{K_{iB}}\right)$$

'Random' mechanism	'Ordered' mechanism
$K_{iA} = K_A$ and $K_{iB} = K_B$	Via E•A $K_{iA} < K_A$ and $K_{iB} > K_B$ Via E•B $K_{iA} > K_A$ and $K_{iB} < K_B$

Figure 7. Catalytic reaction involving a ternary complex.

aminonaphthalene **2f** serves as a strong *N*-ligand that coordinates to the iron in preference to phenol **1b** and *t*-BuOO*t*-Bu.

Scheme 2. Postulated Mechanism for the Oxidative Cross-Coupling between 2,6-Dimethylphenol 1b and *N*-Benzyl-2-aminonaphthalene 2f

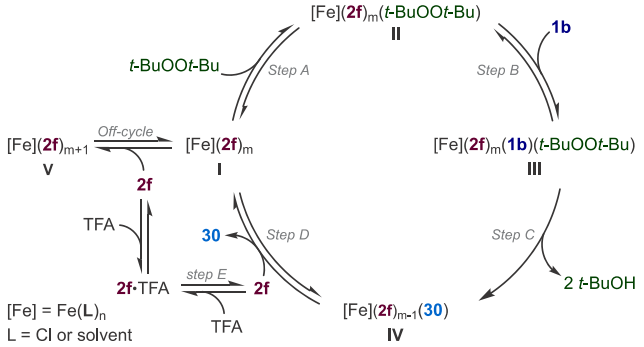

Product inhibition experiments offer useful inputs when deciding the kinetic mechanism of a ternary complex (E·**Q** ⇄ E + **Q**, Figure 7). The experiments were performed by monitoring the formation rate of product **30** in the presence of increasing concentrations of NOBIN **6** or *t*-BuOH. NOBIN **6** was chosen for practical reasons associated with the fact that NOBINs **30** and **6** have different retention times in the HPLC. Figure 8 shows that although *t*-BuOH acts as a weak inhibitor, at saturating values of NOBIN **6**, the catalyst's activity approaches zero. Unsurprisingly, these results indicate that the coupling product acts as a competitive ligand. It is expected that the concentration of complex **IV** ($[Fe]\cdot(\mathbf{2f})_{m-1}(\mathbf{30})$, Scheme 2) builds up as the reaction proceeds; consequently, the velocity of the coupling decreases.

Based on these kinetic results, a detailed mechanistic scheme was postulated and is presented in Scheme 2. The catalytic cycle begins with the reversible binding of the peroxide and the phenol to $[Fe]\cdot(\mathbf{2f})_m$ (**I**), affording complex **III** ($[Fe]\cdot(\mathbf{2f})_m\cdot(\mathbf{1b})\cdot(t\text{-BuOO}t\text{-Bu})$, steps A and B). The homolytic cleavage of the peroxide bond by the iron, followed by an inner-sphere coupling between a phenoxyl radical and a neighboring 2-aminonaphthalene ligand, will afford complex **IV** and two molecules of *t*-BuOH (step C).[2d,e,5b,14] The catalytic cycle is terminated by a reversible ligand exchange process that involves the liberation of *N*,*O*-biaryl product **30**, along with the binding of 2-aminonaphthalene **2f** (step D).

https://dx.doi.org/10.1021/acs.joc.0c00874
J. Org. Chem. 2021, 86, 79−90

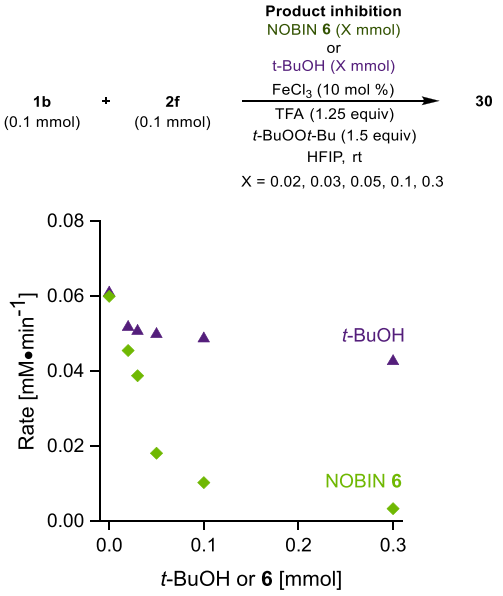

Figure 8. Product inhibition experiments. The effect of [NOBIN **6**] (green diamonds) and [*t*-BuOH] (purple triangles) on the reaction rate. Conditions: phenol **1b** (0.1 mmol), 2-aminonaphthalene **2f** (0.1 mmol), TFA (0.125 mmol), $FeCl_3$ (0.01 mmol), NOBIN **6**, or *t*-BuOH (0.02, 0.03, 0.05, 0.1, and 0.3 mmol), *t*-BuOO*t*-Bu (0.15 mmol), and HFIP (1 mL). The rates of the formation of product **30** in the initial stage of the reaction were determined by HPLC, using mesitylene as the internal standard.

Our study implies that the reaction kinetics is strongly influenced by the relative binding strength of the substrates (2-aminonaphthalene, phenol, and peroxide) and the coupling product to the iron. As mentioned previously, the addition of TFA is mandatory when secondary and tertiary 2-aminonaphthalenes are being reacted. It is expected that TFA, which forms an acid−base adduct with the latter coupling partners, interferes in the net of ligand exchange processes. To clarify the role of the acid, we performed additional sets of kinetic experiments.

The dependence of the initial rate on [TFA] (Figure 6C) revealed that, although no reaction occurs in the absence of the acid, the maximum reactivity is achieved when [**2f**] and [TFA] are equalized (ca. a 1:1 ratio). However, as the acid concentration increases, the reaction velocity diminishes. These results can be rationalized by the existence of ligand-to-metal exchange and acid−base net reactions (Scheme 2). It is suggested that the entire catalytic process is regulated by TFA, which forms an acid−base adduct with **2f**. Accordingly, as the acid concentration increases, the concentration of free 2-aminonaphthalene **2f** drops (step E). Consequently, the off-cycle equilibrium inclines toward complex **I** and the rate accelerates (0.05 M < [TFA] < 0.12 M). On the other hand, at high concentrations of TFA ([TFA] > 0.12 M), the concentration of **2f** diminishes. Consequently, the catalytic cycle termination step (**IV** → **I**, step D), which includes the reversible ligand exchange of the *N*,*O*-biaryl product **30** with **2f**, is discouraged, and the reaction rate declines.

The strength of the TFA-based adduct depends on the basicity of the 2-aminonapthalene molecule. Therefore, different amounts of acid should be used to regulate the coupling of primary, secondary, or tertiary 2-aminonaphthalenes. To support this claim, a set of competitive experiments that studied the coupling of 2-aminonaphthalenes **2a**, **2d**, or **2e** (1 equiv) and 2-naphthol (**1a**, 1.5 equiv) either with or without 2 equiv of TFA were performed (Figure 9). The results show that the addition of TFA to the reaction of **2a**, which is a weaker base in comparison with **2d** and **2e**, negatively affects the reaction rate (Figure 9A). On the other

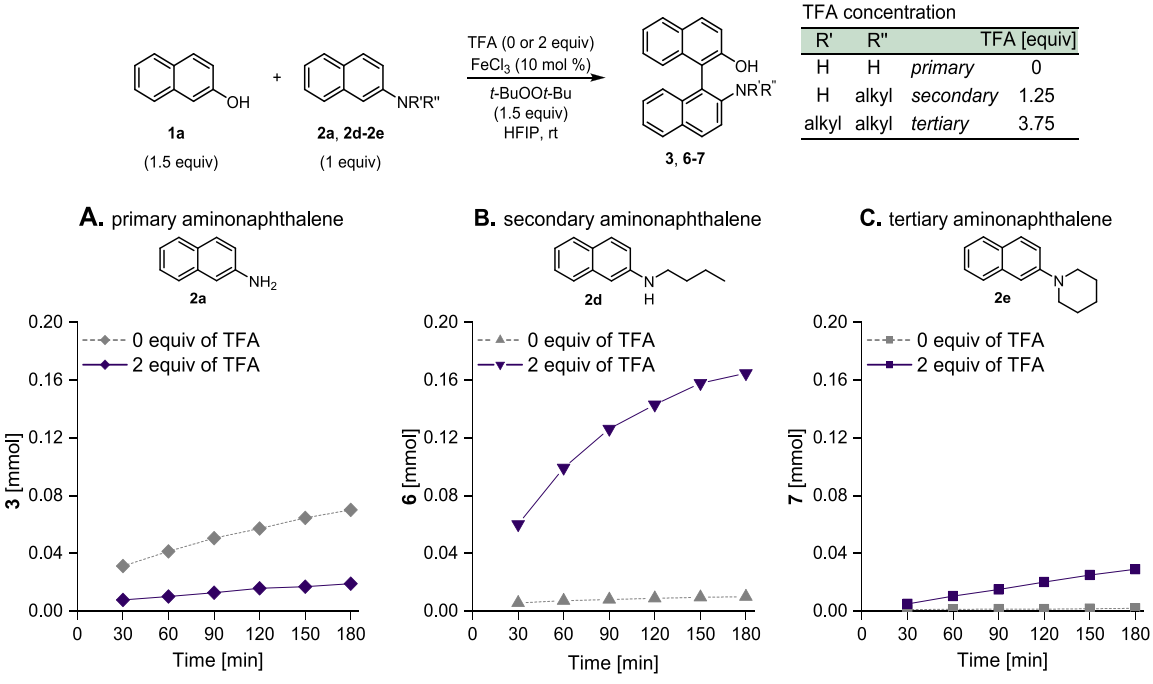

Figure 9. Reaction progress of the oxidative coupling of 2-naphthol **1a** with *N*-substituted-2-aminonaphthalenes (A) **2a**, (B) **2d**, and (C) **2e** with and without TFA (2 equiv). Conditions: 2-naphthol **1a** (0.375 mmol), 2-aminonaphthalene **2a**, **2d**, or **2e** (0.25 mmol), $FeCl_3$ (10 mol %), TFA (0 or 0.5 mmol), *t*-BuOO*t*-Bu (0.375 mmol), and HFIP (0.5 mL) at rt. The formation of products **3**, **6**, or **7** was determined by HPLC, using mesitylene as the internal standard.

https://dx.doi.org/10.1021/acs.joc.0c00874
J. Org. Chem. 2021, 86, 79−90

hand, the reaction of **2d** in the presence of TFA resulted in a significant improvement in the reactivity (Figure 9B) and cross-coupling selectivity (see Figure S3 in the Supporting Information). Finally, tertiary 2-aminonaphthalene **2e** exhibited only a mild improvement in the rate upon the addition of TFA (Figure 9C). This is probably because 2 equiv of TFA are insufficient to regulate the inhibiting off-cycle process. Indeed, almost twice the amount of TFA (3.75 equiv) is needed to ensure efficient cross-coupling, affording NOBIN 7 in 97% yield (Figure 2). Ultimately, the coupling of primary 2-aminonaphthalene takes place at a high efficiency without TFA (see the inserted table, Figure 9), whereas the successful coupling of secondary and tertiary 2-aminonaphthalenes relies on the addition of TFA (1.25 equiv and 3.75 equiv, respectively).

The changes in the catalytic activity at high concentrations of TFA may also be attributed to the generation of iron trifluoroacetate complexes $[Fe(CF_3CO_2)_n(Cl)_m]$. To examine this hypothesis, the $Fe(CF_3CO_2)_3$ complex[22] was prepared and used as a catalyst (10 mol %) in the coupling between **1b** and **2f** (Figure 10). $Fe(CF_3CO_2)_3$ exhibited almost no catalytic

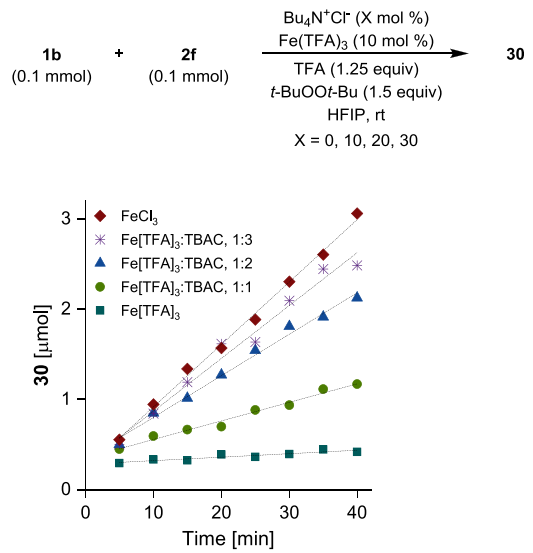

Figure 10. Effect of chloride anions [TBAC] on the catalytic activity of the $Fe(TFA)_3$ catalyst. Conditions: phenol **1b** (0.1 mmol), 2-aminonaphthalene **2f** (0.1 mmol), TFA (0.125 mmol), $FeCl_3$ (0.01 mmol) or $Fe(CF_3CO_2)_3$ and $Bu_4N^+Cl^-$ (0, 10, 20, and 30 mol %), *t*-BuOO*t*-Bu (0.15 mmol), and HFIP (1 mL). The rates of the formation of product **30** in the initial stage of the reaction were determined by HPLC, using mesitylene as the internal standard.

activity. However, the reactivity was enhanced with the addition of 10 mol % of tetrabutylammonium chloride (TBAC). Interestingly, almost a complete recovery of the catalytic activity (in comparison to $FeCl_3$) was achieved with 1:2 and 1:3 iron to chloride ratios. These results suggest that the chloride anions play a key role during the reaction.

CONCLUSIONS

In conclusion, the $FeCl_3$-catalyzed oxidative phenol coupling reaction was applied to combine readily oxidized phenols with primary, secondary, and tertiary 2-aminonaphthalenes. This sustainable and practical method enables a highly selective and efficient synthesis of *N*,*O*-biaryl compounds that are not readily available by other means.

Our mechanistic data, which include control experiments and comprehensive kinetic studies, revealed the existence of a catalytic cycle that involves the formation of a ternary iron complex [Fe]·(**2f**)·(**1b**)·(*t*-BuOO*t*-Bu) (**III**) from $[Fe]\cdot(\mathbf{2f})_m$ (**I**) by the sequential binding of peroxide and phenol. The irreversible rate-determining oxidative coupling step comprises the conversion of complex **III** to **IV** ($[Fe]\cdot(\mathbf{2f})_{m-1}(\mathbf{30})$) and the liberation of two molecules of *t*-BuOH. In this transformation, a reaction between an iron-bound phenoxyl radical and a neighboring 2-aminonaphthalene ligand takes place. The velocity of the reaction is regulated by a net of acid−base and ligand exchange processes. The reaction rate is highly sensitive to changes in the concentrations of the substrates (2-aminonaphthalene, phenol, and peroxide), the acid (TFA), and the *N*,*O*-biaryl product. Furthermore, the chloride anions have a strong effect on the reaction efficiency. Finally, this study is a part of our laboratory ongoing research that aims to develop selective oxidative cross-coupling reactions for the coupling of anilines by first-row metal catalysts.

EXPERIMENTAL SECTION

General Methods. All reagents were of reagent-grade quality, purchased commercially from Sigma-Aldrich, Alfa-Aesar, or Fluka, and used without further purification. $FeCl_3$ (anhydrous 98%) was purchased from Strem Chemicals. Purification by column chromatography was performed on Merck chromatographic silica gel (40−63 μm). Thin-layer chromatography (TLC) analyses were performed using Merck silica gel glass plates 60 F254. NMR spectra were recorded on Bruker DPX400 or DMX500 instruments; chemical shifts are relative to Me_4Si as the internal standard or to the residual solvent peak. High-resolution mass spectrometry (HRMS) data were obtained using an LTQ Orbitrap XL ETD (Thermo Fisher Scientific, Germany and USA) high-resolution mass spectrometer. The reactions in the microwave were performed using a CEM Discover SP microwave synthesizer. IR spectra were recorded on a JASCO FT/IR-460 Plus FT-IR instrument. HPLC analysis was carried out on an Agilent 1260 instrument equipped with a G4212-60008 photodiode array detector and an Agilent reverse phase ZORBAX Eclipse plus C18 3.5 μm column (4.6 × 100 mm).

General Procedures for the Synthesis of *N*-Alkyl-2-aminonaphthalenes. ***Method A.*** A mixture of 2-naphthol derivative (1 equiv) and alkyl/arylamine (5 equiv) was irradiated in a microwave for 20 h (sealed reaction vessel, temperature of 275 °C was monitored by using an external surface sensor and a power of 200 W). The volatiles were removed under reduced pressure, and the crude residue was further purified by silica-gel column chromatography (silica gel 40−63 μm). This method was used for the preparation of 2-aminonaphthalene derivatives **2d**, **2e**, **2i**, **2j**, **2n**, and **2o**.

Method B.[23] A mixture of 2-aminonaphthalene (1 equiv) and benzaldehyde (1.1 equiv) was stirred in methanol (0.17 M) for 1 h, and then $NaBH_4$ (1.5 equiv) was added. The reaction was stirred for 20 min, and the volatiles were removed under reduced pressure. NaOH (1 M, 30 mL) was added and extracted with diethyl ether (3 × 20 mL). The combined organic phase was dried over $MgSO_4$ and evaporated under reduced pressure. The crude residue was further purified by silica-gel column chromatography (silica gel 40−63 μm). This method was used for the preparation of 2-aminonaphthalene derivatives **2f**, **2g**, **2h**, **2k**, **2l**, **2 m**, and **2p**.

*N-Heptyl-3-methoxy-2-aminonaphthalene (**2i**).* This compound was prepared from 3-methoxy-2-naphthol (1 g, 5.74 mmol) and 1-heptylamine (4.24 mL, 28.7 mmol) according to method A. The crude residue was purified by silica-gel column chromatography (hexane/ethyl acetate 99:1) to afford compound **2i** (1.49 g, 96% yield) as a dark red oil. ^1H NMR ($CDCl_3$, 400 MHz): δ 0.93 (t, 3H, J = 6.9 Hz), 1.25−1.56 (m, 8H), 1.75 (quin, 2H, J = 7.2 Hz), 3.24 (t, 2H, J = 7.2 Hz), 3.98 (s, 3H), 6.79 (s, 1H), 7.02 (s, 1H), 7.21 (ddt, 1H, J = 8.0, 7.0, 1.2 Hz), 7.29 (ddt, 1H, J = 8.0, 6.9, 1.2 Hz), 7.62 (d,

https://dx.doi.org/10.1021/acs.joc.0c00874
J. Org. Chem. 2021, 86, 79−90

1H, J = 4.1 Hz), 7.64 (d, 1H, J = 4.0 Hz). $^{13}C\{^1H\}$ NMR ($CDCl_3$, 100 MHz): δ 14.2, 22.8, 27.4, 29.3, 29.4, 32.0, 43.8, 55.6, 103.4, 104.5, 122.1, 124.1, 125.4, 126.4, 127.2, 130.6, 138.8, 148.2. HRMS (ESI) m/z: $[M + H]^+$ calcd for $C_{18}H_{26}NO$ 272.2009, found 272.2014.

*N-Heptyl-6-methoxy-2-aminonaphthalene (**2j**).* This compound was prepared from 6-methoxy-2-naphthol (697 mg, 4 mmol) and 1-heptylamine (2.84 mL, 20 mmol) according to method A. The crude residue was purified by silica-gel column chromatography (hexane/ethyl acetate 98:2) to afford compound **2j** (787 mg, 72% yield) as a dark gray solid. ^1H NMR ($CDCl_3$, 400 MHz): δ 0.90 (t, 3H, J = 6.9 Hz), 1.21−1.53 (m, 8H), 1.68 (quin, 2H, J = 8.0 Hz), 3.19 (t, 2H, J = 8.0 Hz), 3.88 (s, 3H), 6.83 (d, 1H, J = 2.3 Hz), 6.90 (dd, 1H, J = 8.7, 2.4 Hz), 7.03 (d, 1H, J = 2.5 Hz), 7.07 (dd, 1H, J = 8.9, 2.6 Hz), 7.53 (s, 1H), 7.55 (s, 1H). $^{13}C\{^1H\}$ NMR ($CDCl_3$, 100 MHz): δ 14.3, 22.8, 27.3, 29.3, 29.5, 32.0, 44.7, 55.4, 105.6, 106.3, 118.6, 118.8, 127.6, 127.8, 128.3, 130.6, 144.4, 155.2. HRMS (ESI) m/z: $[M + H]^+$ calcd for $C_{18}H_{26}NO$ 272.2009, found 272.2003.

*N-(4-t-Butylbenzyl)-2-aminonaphthalene (**2m**).* This compound was prepared from 2-naphthylamine (716 mg, 5 mmol) and 4-*t*-butylbenzaldehyde (0.92 mL, 5.5 mmol) according to method B. The crude residue was purified by silica-gel column chromatography (hexane/ethyl acetate 98:2) to afford compound **2m** (928 mg, 64% yield) as a white solid. ^1H NMR ($CDCl_3$, 400 MHz): δ 1.34 (s, 9H), 4.41 (s, 2H), 6.87 (d, 1H, J = 2.3 Hz), 6.92 (dd, 1H, J = 8.7, 2.4 Hz), 7.20 (ddd, 1H, J = 8.1, 6.8, 1.2 Hz), 7.33−7.42 (m, 5H), 7.61 (dd, 1H, J = 8.3, 0.7 Hz), 7.64 (d, 1H, J = 9.0 Hz), 7.68 (d, 1H, J = 8.2 Hz). $^{13}C\{^1H\}$ NMR ($CDCl_3$, 100 MHz): δ 31.5, 34.7, 48.2, 104.7, 118.0, 122.1, 125.8, 126.1, 126.4, 127.6, 127.7, 127.8, 129.1, 135.4, 136.2, 146.0, 150.5. HRMS (ESI) m/z: $[M + H]^+$ calcd for $C_{21}H_{24}N$ 290.1903, found 290.1899.

*N-Benzyl-3-methoxy-2-aminonaphthalene (**2n**).* This compound was prepared from 3-methoxy-2-naphthol (1 g, 5.74 mmol) and benzylamine (3.14 mL, 28.7 mmol) according to method A. The crude residue was purified by silica-gel column chromatography (hexane/ethyl acetate 99:1) to afford compound **2n** (470 mg, 31% yield) as a white solid. ^1H NMR ($CDCl_3$, 400 MHz): δ 3.99 (s, 3H), 4.48 (s, 2H), 4.94 (bs, 1H), 6.82 (s, 1H), 7.06 (s, 1H), 7.20−7.35 (m, 3H), 7.39 (t, 2H, J = 7.3 Hz), 7.46 (d, 2H, J = 7.5 Hz), 7.59 (d, 1H, J = 8.0 Hz), 7.65 (d, 1H, J = 7.8 Hz). $^{13}C\{^1H\}$ NMR ($CDCl_3$, 100 MHz): δ 48.1, 55.6, 103.9, 104.7, 122.4, 124.1, 125.6, 126.4, 127.4 (× 2C), 127.8, 128.8, 130.4, 138.5, 139.2, 148.2. HRMS (ESI) m/z: $[M + H]^+$ calcd for $C_{18}H_{18}NO$ 264.1383, found 264.1382.

General Procedure for the Oxidative Cross-Coupling of 2-Naphthols/Phenols with 2-Aminonaphthalenes. To a stirred solution of 2-naphthol or phenol derivative (1.5 equiv), 2-aminonaphthalene derivative (1 equiv), TFA (1.25 equiv), and $FeCl_3$ (10 mol %) in HFIP (0.5 M), *t*-BuOO*t*-Bu (1.5 equiv) was added dropwise at room temperature. The reaction was stirred for 24 h until full consumption of 2-aminonaphthalene. The volatiles were removed under reduced pressure, and the crude was further purified by silica-gel column chromatography (silica gel 40−63 μm), affording pure NOBIN products.

*2-Amino-2′-hydroxy-1,1′-binaphthyl (**3**).* 2-Naphthol **1a** (54.1 mg, 0.375 mmol) and 2-aminonaphthalene **2a** (35.8 mg, 0.25 mmol) were reacted according to the general procedure. In this reaction, TFA was not added. The crude residue was purified by column chromatography (hexane/ethyl acetate 90:10) to afford compound **3** (58.5 mg, 82% yield) as a pale brown solid. ^1H NMR ($CDCl_3$, 400 MHz): δ 7.03−7.08 (m, 1H), 7.13 (d, 1H, J = 8.8 Hz), 7.16−7.20 (m, 1H), 7.20−7.30 (m, 3H), 7.33−7.38 (m, 1H), 7.39 (d, 1H, J = 8.9 Hz), 7.81 (dd, 1H, J = 7.4, 1.9 Hz), 7.85 (d, 1H, J = 8.6 Hz), 7.89 (d, 1H, J = 8.0 Hz), 7.93 (d, 1H, J = 8.8 Hz). $^{13}C\{^1H\}$ NMR ($CDCl_3$, 100 MHz): δ 108.7, 114.4, 117.8, 118.3, 122.9, 123.8, 123.9, 124.7, 127.1, 127.4, 128.4 (x 3C), 129.6, 130.5, 130.7, 133.3, 134.2, 143.8, 151.9. HRMS (ESI) m/z: $[M-H]^+$ calcd for $C_{20}H_{14}NO$ 284.1070, found 284.1058.

*2′-(Butylamino)-[1,1′-binaphthalen]-2-ol (**6**).* 2-Naphthol **1a** (54.1 mg, 0.375 mmol) and *N*-butyl-2-aminonaphthalene **2d** (49.8 mg, 0.25 mmol) were reacted according to the general procedure. The crude residue was purified by column chromatography (hexane/ethyl acetate 95:5) to afford compound **6** (67.4 mg, 79% yield) as a yellow syrup. ^1H NMR ($CDCl_3$, 400 MHz): δ 0.80 (t, 3H, J = 7.3 Hz), 1.11−1.23 (m, 2H), 1.33−1.44 (m, 2H), 3.16 (td, 2H, J = 7.1, 1.9 Hz), 6.92−6.98 (m, 1H), 7.14 (d, 1H, J = 8.6 Hz), 7.16−7.22 (m, 2H), 7.24 (ddd, 2H, J = 8.0, 4.7, 1.7 Hz), 7.30−7.35 (m, 1H), 7.37 (d, 1H, J = 8.9 Hz), 7.75−7.79 (m, 1H), 7.86 (d, 1H, J = 8.0 Hz), 7.90 (d, 1H, J = 5.5 Hz), 7.92 (d, 1H, J = 5.4 Hz). $^{13}C\{^1H\}$ NMR ($CDCl_3$, 100 MHz): δ 13.9, 20.0, 31.9, 43.7, 107.9, 114.1, 114.3, 117.8, 122.2, 123.6, 123.8, 124.7, 127.0, 127.3, 127.5, 128.3, 128.4, 129.7, 130.5, 130.8, 133.6, 134.3, 145.6, 152.1. HRMS (ESI) m/z: $[M + H]^+$ calcd for $C_{24}H_{24}NO$ 342.1852, found 342.1845.

*2′-(Piperidin-1-yl)-[1,1′-binaphthalen]-2-ol (**7**).* 2-Naphthol **1a** (54.1 mg, 0.375 mmol) and piperidino-2-naphthalene **2e** (52.8 mg, 0.25 mmol) were reacted according to the general procedure. In this reaction, addition of 2-naphthol (1.5 equiv), TFA (2 × 1.25 equiv), and *t*-BuOO*t*-Bu (2 × 1.5 equiv) was needed to ensure full consumption of 2-aminonaphthalene. Then, the reaction was quenched by the addition of CH_2Cl_2 and sat. $NaHCO_3$. The organic phase was separated, dried over $MgSO_4$, and evaporated under reduced pressure. The crude residue was purified by column chromatography (hexane/ethyl acetate 98:2) to afford compound **7** (85.8 mg, 97% yield) as a brown solid. ^1H NMR ($CDCl_3$, 400 MHz): δ 1.46 (s, 6H), 2.88−3.06 (m, 4H), 7.09 (dd, 2H, J = 8.0, 0.5 Hz), 7.13−7.23 (m, 2H), 7.34 (dtd, 2H, J = 8.0, 6.6, 1.3 Hz), 7.46 (d, 1H, J = 8.8 Hz), 7.51 (d, 1H, J = 8.9 Hz), 7.86 (dd, 1H, J = 8.2, 0.5 Hz), 7.88−7.91 (m, 1H), 7.91 (d, 1H, J = 8.9 Hz), 7.98 (d, 1H, J = 8.8 Hz), 8.26 (bs, 1H). $^{13}C\{^1H\}$ NMR ($CDCl_3$, 100 MHz): δ 24.1, 26.4, 53.5, 118.7, 118.8, 120.5, 123.2, 124.6, 125.3, 126.1, 126.2, 126.3, 126.6, 128.0, 128.3, 129.4, 129.7, 129.9, 130.6, 133.8, 134.3, 149.1, 151.8. IR (KBr pellet): 3431 (s, broad), 2934 (s), 1224 (s), 749 (s) cm^{-1}. HRMS (ESI) m/z: $[M + H]^+$ calcd for $C_{25}H_{24}NO$ 354.1852, found 354.1847.

*2′-((4-Chlorobenzyl)amino)-[1,1′-binaphthalen]-2-ol (**8**).* 2-Naphthol **1a** (54.1 mg, 0.375 mmol) and *N*-(4-chlorobenzyl)-2-aminonaphthalene **2 g** (66.9 mg, 0.25 mmol) were reacted according to the general procedure. The crude residue was purified by column chromatography (hexane/ethyl acetate 85:15) to afford compound **8** (94.7 mg, 92% yield) as a brown solid. ^1H NMR ($CDCl_3$, 400 MHz): δ 4.36 (s, 2H), 5.16 (bs, 1H), 6.97−7.03 (m, 1H), 7.09 (d, 1H, J = 9.0 Hz), 7.12 (d, 2H, J = 8.4 Hz), 7.17 (dd, 1H, J = 8.3, 0.4 Hz), 7.18−7.25 (m, 4H), 7.30 (ddd, 1H, J = 8.2, 6.8, 1.4 Hz), 7.37 (ddd, 1H, J = 8.1, 6.8, 1.3 Hz), 7.41 (d, 1H, J = 8.9 Hz), 7.75−7.80 (m, 1H), 7.84 (d, 1H, J = 8.8 Hz), 7.90 (d, 1H, J = 7.9 Hz), 7.95 (d, 1H, J = 8.9 Hz). $^{13}C\{^1H\}$ NMR ($CDCl_3$, 100 MHz): δ 47.0, 108.5, 114.0, 117.8, 122.6, 123.6, 123.9, 124.7, 127.2, 127.5, 127.8, 128.2, 128.4, 128.5, 128.9 (x 2C), 129.7, 130.7, 130.9, 132.9, 133.5, 134.2, 138.1, 144.7, 152.2. HRMS (ESI) m/z: $[M + H]^+$ calcd for $C_{27}H_{21}ClNO$ 410.1306, found 410.1299.

*6-Bromo-2′-((3-hydroxy-4-methoxybenzyl)amino)-[1,1′-binaphthalen]-2-ol (**9**).* 6-Bromo-2-naphthol (83.6 mg, 0.375 mmol) and *N*-(3-hydroxy-4-methoxybenzyl)-2-aminonaphthalene **2h** (69.8 mg, 0.25 mmol) were reacted according to the general procedure. The crude residue was purified by column chromatography (hexane/ethyl acetate 95:5) to afford compound **9** (100.4 mg, 80% yield) as a brown solid. ^1H NMR ($CDCl_3$, 400 MHz): δ 3.82 (s, 3H), 4.14 (bs, 1H), 4.29 (s, 2H), 5.28 (bs, 1H), 5.58 (s, 1H), 6.64 (dd, 1H, J = 8.2, 2.0 Hz), 6.71 (d, 1H, J = 8.2 Hz), 6.76 (d, 1H, J = 2.0 Hz), 6.90−6.96 (m, 1H), 7.05 (d, 1H, J = 9.0 Hz), 7.16 (d, 1H, J = 9.0 Hz), 7.18−7.25 (m, 2H), 7.34 (dd, 1H, J = 9.0, 2.0 Hz), 7.41 (d, 1H, J = 8.9 Hz), 7.74−7.79 (m, 1H), 7.84 (d, 2H, J = 8.8 Hz), 8.03 (d, 1H, J = 2.0 Hz). $^{13}C\{^1H\}$ NMR ($CDCl_3$, 100 MHz): δ 47.2, 56.1, 107.6, 110.8, 113.2, 114.4, 114.6, 117.6, 118.2, 119.0, 122.5, 123.3, 126.7, 127.5, 127.7, 128.4, 129.6, 130.3, 130.4, 130.8, 131.0, 132.1, 132.6, 134.1, 145.1, 145.8 (x 2C), 152.5. HRMS (ESI) m/z: $[M + H]^+$ calcd for $C_{28}H_{23}BrNO_3$ 500.0856, found 500.0856.

*3-Bromo-2′-((3-hydroxy-4-methoxybenzyl)amino)-[1,1′-binaphthalen]-2-ol (**10**).* 3-Bromo-2-naphthol (83.6 mg, 0.375 mmol) and *N*-(3-hydroxy-4-methoxybenzyl)-2-aminonaphthalene **2 h** (69.8 mg, 0.25 mmol) were reacted according to the general procedure. The crude residue was purified by column chromatography (hexane/ethyl

https://dx.doi.org/10.1021/acs.joc.0c00874
J. Org. Chem. 2021, 86, 79−90

acetate 95:5) to afford compound **10** (101.4 mg, 81% yield) as a brown solid. ^{1}H NMR ($CDCl_3$, 400 MHz): δ 3.81 (s, 3H), 3.95 (s, 1H), 4.30 (s, 2H), 5.58 (bs, 1H), 6.66 (dd, 1H, J = 8.3, 1.6 Hz), 6.71 (d, 1H, J = 8.2 Hz), 6.76 (d, 1H, J = 1.7 Hz), 6.95 (dd, 1H, J = 8.7, 4.5 Hz), 7.13−7.24 (m, 4H), 7.28−7.36 (m, 1H), 7.36−7.45 (m, 1H), 7.75−7.79 (m, 1H), 7.81 (d, 1H, J = 8.1 Hz), 7.85 (d, 1H, J = 9.0 Hz), 8.25 (s, 1H). ^{13}C{^{1}H} NMR ($CDCl_3$, 100 MHz): δ 47.3, 56.0, 108.5, 110.3, 110.8, 111.9, 113.2, 114.4, 116.2, 118.2, 122.4, 123.3, 124.8, 125.0, 127.4, 127.5, 127.6, 128.4, 130.2, 130.9, 132.6, 132.8 (x 2C), 133.8, 144.8, 145.7, 145.8, 148.7. HRMS (ESI) m/z: $[M + H]^+$ calcd for $C_{28}H_{23}BrNO_3$ 500.0856, found 500.0880.

*Methyl 2′-(Heptylamino)-2-hydroxy-3′-methoxy-[1,1′-binaphthalene]-3-carboxylate (**11**).* Methyl 3-hydroxy-2-naphthoate (75.8 mg, 0.375 mmol) and *N*-heptyl-3-methoxy-2-aminonaphthalene **2i** (67.8 mg, 0.25 mmol) were reacted according to the general procedure. The crude residue was purified by column chromatography (hexane/ethyl acetate 85:15) to afford compound **11** (81.9 mg, 70% yield) as a yellow solid. ^{1}H NMR ($CDCl_3$, 400 MHz): δ 0.84 (t, 3H, J = 7.2 Hz), 0.88−1.12 (m, 6H), 1.22 (ddd, 4H, J = 21.9, 16.5, 9.1 Hz), 2.52−2.71 (m, 1H), 2.71−2.86 (m, 1H), 4.06 (s, 3H), 4.07 (s, 3H), 6.98 (d, 1H, J = 8.4 Hz), 7.08 (t, 1H, J = 7.6 Hz), 7.23 (d, 2H, J = 4.7 Hz), 7.28 (d, 1H, J = 4.3 Hz), 7.35 (dd, 2H, J = 6.1, 2.4 Hz), 7.74 (d, 1H, J = 8.0 Hz), 7.86−7.99 (m, 1H), 8.70 (s, 1H). ^{13}C{^{1}H} NMR ($CDCl_3$, 100 MHz): δ 14.1, 22.6, 26.7, 28.9, 30.7, 31.8, 46.6, 52.8, 55.6, 105.8, 114.0, 115.7, 119.8, 123.2, 124.0, 124.2 (x 2C), 125.5, 126.8, 127.1, 129.0, 129.4, 129.7 (x 2C), 132.7, 137.7, 138.2, 150.3, 154.4, 170.6. HRMS (ESI) m/z: $[M + H]^+$ calcd for $C_{30}H_{34}NO_4$ 472.2482, found 472.2477.

*Methyl 2′-(Heptylamino)-2-hydroxy-6′-methoxy-[1,1′-binaphthalene]-6-carboxylate (**12**).* Methyl 6-hydroxy-2-naphthoate (75.8 mg, 0.375 mmol) and *N*-heptyl-6-methoxy-2-aminonaphthalene **2j** (67.8 mg, 0.25 mmol) were reacted according to the general procedure. The crude residue was purified by column chromatography (hexane/ethyl acetate 90:10) to afford compound **12** (111.1 mg, 94% yield) as a brown solid. ^{1}H NMR ($CDCl_3$, 400 MHz): δ 0.83 (t, 3H, J = 7.0 Hz), 1.03−1.24 (m, 8H), 1.33−1.46 (m, 2H), 3.14 (t, 2H, J = 7.1 Hz), 3.88 (s, 3H), 3.94 (s, 3H), 6.84 (d, 1H, J = 9.2 Hz), 6.90 (dd, 1H, J = 9.2, 2.6 Hz), 7.15 (d, 1H, J = 2.6 Hz), 7.16 (d, 1H, J = 8.9 Hz), 7.24 (d, 1H, J = 9.0 Hz), 7.43 (d, 1H, J = 8.9 Hz), 7.79−7.88 (m, 2H), 8.03 (d, 1H, J = 8.9 Hz), 8.63 (d, 1H, J = 1.6 Hz). ^{13}C{^{1}H} NMR ($CDCl_3$, 100 MHz): δ 14.2, 22.6, 26.8, 29.0, 29.7, 31.8, 44.2, 52.2, 55.5, 106.9, 108.0, 114.8, 114.9, 118.7, 119.9, 124.9, 125.0, 125.4, 126.5, 128.4, 128.6, 129.5, 129.8, 131.6, 132.0, 136.1, 144.0, 154.3, 155.4, 167.4. HRMS (ESI) m/z: $[M + H]^+$ calcd for $C_{30}H_{34}NO_4$ 472.2482, found 472.2459.

*2′-(Cinnamylamino)-6-isopropyl-[1,1′-binaphthalen]-2-ol (**13**).* 6-Isopropyl-2-naphthol[5c] (69.8 mg, 0.375 mmol) and *N*-cinnamyl-2-aminonaphthalene **2k** (64.8 mg, 0.25 mmol) were reacted according to the general procedure. The crude residue was purified by column chromatography (hexane/ethyl acetate 95:5) to afford compound **13** (66.3 mg, 60% yield) as a yellow solid. ^{1}H NMR ($CDCl_3$, 400 MHz): δ 1.32 (dd, 6H, J = 6.9, 1.9 Hz), 3.03 (hept, 1H, J = 6.9 Hz), 4.00 (d, 2H, J = 4.5 Hz), 5.10 (bs, 1H), 6.15 (dt, 1H, J = 15.9, 4.8 Hz), 6.44 (d, 1H, J = 15.9 Hz), 7.00−7.03 (m, 1H), 7.13 (d, 1H, J = 8.7 Hz), 7.17−7.24 (m, 4H), 7.26 (d, 3H, J = 2.3 Hz), 7.28 (d, 2H, J = 9.1 Hz), 7.37 (d, 1H, J = 8.9 Hz), 7.69 (d, 1H, J = 1.4 Hz), 7.78−7.81 (m, 1H), 7.87−7.94 (m, 2H). ^{13}C{^{1}H} NMR ($CDCl_3$, 100 MHz): δ 24.0, 24.1, 34.0, 45.7, 108.7, 114.1, 114.3, 117.7, 122.4, 123.7, 124.7 (x 2C), 126.4, 127.0, 127.2, 127.3, 127.6, 127.8, 128.3, 128.6, 129.9, 130.2, 130.8, 131.1, 132.0, 134.3, 136.8, 144.2, 145.1, 151.6. HRMS (ESI) m/z: $[M + H]^+$ calcd for $C_{32}H_{30}NO$ 444.2322, found 444.2319.

*2′-((4-Methoxybenzyl)amino)-5,6,7,8-tetrahydro-[1,1′-binaphthalen]-2-ol (**14**).* 5,6,7,8-Tetrahydro-2-naphthol (55.6 mg, 0.375 mmol) and *N*-(4-methoxybenzyl)-2-aminonaphthalene **2l** (65.8 mg, 0.25 mmol) were reacted according to the general procedure. The crude residue was purified by column chromatography (hexane/ethyl acetate 95:5) to afford compound **14** (88.1 mg, 86% yield) as a brown solid. ^{1}H NMR ($CDCl_3$, 500 MHz): δ 1.80−1.89 (m, 4H), 2.68−2.90 (m, 4H), 3.78 (s, 3H), 4.40 (s, 2H), 6.85 (ddd, 3H, J = 6.8, 5.3, 2.8 Hz), 6.91 (s, 1H), 7.09−7.15 (m, 1H), 7.18−7.25 (m, 3H), 7.29−7.33 (m, 2H), 7.72 (d, 1H, J = 8.1 Hz), 7.75 (d, 1H, J = 9.0 Hz). ^{13}C{^{1}H} NMR ($CDCl_3$, 100 MHz): δ 23.3, 23.6, 28.7, 29.6, 47.6, 55.4, 114.2, 114.4, 116.0, 119.3, 122.4, 123.1, 123.9, 127.0, 127.7, 128.2, 128.3, 130.1, 130.2, 131.4, 132.3, 134.0, 139.2, 144.0, 151.7, 158.9. HRMS (ESI) m/z: $[M + H]^+$ calcd for $C_{28}H_{28}NO_2$ 410.2115, found 410.2104.

*2′-((4-(t-Butyl)benzyl)amino)-6-(4-(t-butyl)phenyl)-[1,1′-binaphthalen]-2-ol (**15**).* 6-(4-*t*-Butylphenyl)-2-naphthol[5c] (103.6 mg, 0.375 mmol) and *N*-(4-*t*-butylbenzyl)-2-aminonaphthalene **2m** (72.4 mg, 0.25 mmol) were reacted according to the general procedure. The crude residue was purified by column chromatography (hexane/ethyl acetate 98:2) to afford compound **15** (99.9 mg, 71% yield) as a brown solid. ^{1}H NMR ($CDCl_3$, 400 MHz): δ 1.27 (s, 9H), 1.38 (s, 9H), 4.33−4.46 (m, 2H), 7.05 (dd, 1H, J = 6.0, 3.3 Hz), 7.13 (d, 2H, J = 8.1 Hz), 7.18−7.24 (m, 3H), 7.27 (d, 3H, J = 8.1 Hz), 7.43 (d, 1H, J = 8.9 Hz), 7.50 (d, 2H, J = 8.1 Hz), 7.57 (d, 1H, J = 8.7 Hz), 7.63 (d, 2H, J = 8.2 Hz), 7.78 (dd, 1H, J = 5.9, 3.4 Hz), 7.87 (d, 1H, J = 9.1 Hz), 7.99 (d, 1H, J = 9.0 Hz), 8.08 (s, 1H). ^{13}C{^{1}H} NMR ($CDCl_3$, 100 MHz): δ 31.5 (x 2C), 34.6, 34.7, 47.3, 108.2, 114.2, 114.4, 118.2, 122.4, 123.6, 125.3, 125.6, 125.9, 126.2, 126.6, 126.8, 127.0, 127.4, 127.7, 128.4, 130.0, 130.9 (x 2C), 132.7, 134.2, 136.4, 136.5, 138.3, 145.2, 150.1, 150.3, 152.2. HRMS (ESI) m/z: $[M + H]^+$ calcd for $C_{41}H_{42}NO$ 564.3261, found 564.3267.

*2′-(Benzylamino)-3-(4-(t-butyl)phenyl)-[1,1′-binaphthalen]-2-ol (**16**).* 3-(4-*t*-Butylphenyl)-2-naphthol[12] (103.6 mg, 0.375 mmol) and *N*-benzyl-2-aminonaphthalene **2f** (58.3 mg, 0.25 mmol) were reacted according to the general procedure. The crude residue was purified by column chromatography (hexane/ethyl acetate 98:2) to afford compound **16** (80.1 mg, 63% yield) as a brown solid. ^{1}H NMR ($CDCl_3$, 400 MHz): δ 1.39 (s, 9H), 4.43 (s, 2H), 7.05−7.11 (m, 1H), 7.14−7.27 (m, 9H), 7.27−7.32 (m, 1H), 7.38 (ddd, 1H, J = 8.1, 6.8, 1.3 Hz), 7.49−7.55 (m, 2H), 7.69−7.74 (m, 2H), 7.75−7.81 (m, 1H), 7.86 (d, 1H, J = 8.6 Hz), 7.91 (dd, 1H, J = 8.0, 0.5 Hz), 8.00 (s, 1H). ^{13}C{^{1}H} NMR ($CDCl_3$, 100 MHz): δ 31.5, 34.8, 47.7, 108.6, 114.3, 114.9, 122.4, 123.7, 124.1, 124.7, 125.4, 126.9 (x 2C), 127.2, 127.4, 127.7, 128.3, 128.5, 128.7, 129.4, 129.8, 130.6, 130.7, 130.9, 132.9, 134.2, 135.1, 139.6, 145.1, 149.9, 150.6. HRMS (ESI) m/z: $[M + H]^+$ calcd for $C_{37}H_{34}NO$ 508.2635, found 508.2628.

*2′-(Benzylamino)-3-(4-(t-butyl)phenyl)-3′-methoxy-[1,1′-binaphthalen]-2-ol (**17**).* 3-(4-*t*-Butylphenyl)-2-naphthol[12] (103.6 mg, 0.375 mmol) and *N*-benzyl-3-methoxy-2-aminonaphthalene **2n** (65.8 mg, 0.25 mmol) were reacted according to the general procedure. The crude residue was purified by column chromatography (hexane/ethyl acetate 85:15) to afford compound **17** (122.7 mg, 91% yield) as a brown solid. ^{1}H NMR ($CDCl_3$, 400 MHz): δ 1.46 (s, 9H), 3.95 (q, 2H, J = 13.6 Hz), 4.08 (s, 3H), 6.95−7.07 (m, 2H), 7.19 (dt, 4H, J = 16.2, 7.3 Hz), 7.23−7.45 (m, 6H), 7.53−7.64 (m, 2H), 7.71−7.85 (m, 3H), 7.88−8.12 (m, 2H). ^{13}C{^{1}H} NMR ($CDCl_3$, 100 MHz): δ 31.5, 34.7, 50.8, 55.9, 106.6, 114.4, 117.3, 123.9, 124.0, 124.5, 124.8, 125.3, 125.4, 126.7, 126.8, 127.1, 127.8, 128.3, 128.4, 129.3, 129.4 (x 2C), 129.5, 130.4, 130.8, 133.5, 135.3, 138.5, 139.9, 149.6, 150.0, 150.4. HRMS (ESI) m/z: $[M + H]^+$ calcd for $C_{38}H_{36}NO_2$ 538.2741, found 538.2748.

*2,6-Dimethyl-4-(2-(piperidin-1-yl)naphthalen-1-yl)phenol (**18**).* 2,6-Dimethylphenol **1b** (45.8 mg, 0.375 mmol) and piperidino-2-naphthalene **2e** (52.8 mg, 0.25 mmol) were reacted according to the general procedure. In this reaction, addition of TFA (1.25 equiv) and *t*-BuOO*t*-Bu (1.5 equiv) was needed to ensure full consumption of 2-aminonaphthalene. Then, the reaction was quenched by the addition of CH_2Cl_2 and sat. $NaHCO_3$. The organic phase was separated, dried over $MgSO_4$, and evaporated under reduced pressure. The crude residue was purified by column chromatography (hexane/ethyl acetate 95:5) to afford compound **18** (78.6 mg, 95% yield) as a pale brown solid. ^{1}H NMR ($CDCl_3$, 400 MHz): δ 1.35−1.50 (m, 6H), 2.35 (s, 6H), 2.83−2.92 (m, 4H), 4.71 (bs, 1H), 7.08 (s, 2H), 7.29−7.37 (m, 2H), 7.39 (d, 1H, J = 8.8 Hz), 7.70−7.76 (m, 1H), 7.77−7.84 (m, 2H). ^{13}C{^{1}H} NMR ($CDCl_3$, 100 MHz): δ 16.1, 24.5, 26.5, 53.0, 120.4, 122.4, 123.7, 125.7, 125.8, 127.8, 128.1, 130.2, 130.3, 131.4, 131.6, 133.7, 149.3, 150.8. HRMS (ESI) m/z: $[M + H]^+$

https://dx.doi.org/10.1021/acs.joc.0c00874
J. Org. Chem. 2021, 86, 79−90

calcd for $C_{23}H_{26}NO$ 332.2009, found 332.2009. IR (KBr pellet): 3566 (s), 2932 (s), 1231 (s), 749 (s) cm^{-1}.

*2-(2-(Benzylamino)-3-methoxynaphthalen-1-yl)-3,5,6-trimethylphenol (**19**).* 2,3,5-Trimethylphenol (51.1 mg, 0.375 mmol) and *N*-benzyl-3-methoxy-2-aminonaphthalene **2n** (65.8 mg, 0.25 mmol) were reacted according to the general procedure. The crude residue was purified by column chromatography (hexane/ethyl acetate 95:5) to afford compound **19** (60.6 mg, 61% yield) as a pale brown solid. ^1H NMR ($CDCl_3$, 400 MHz): δ 1.89 (s, 3H), 2.23 (s, 3H), 2.36 (s, 3H), 4.04 (s, 3H), 4.05 (d, 2H, J = 2.1 Hz), 6.77 (s, 1H), 7.13−7.34 (m, 9H), 7.72 (dd, 1H, J = 7.8, 0.6 Hz). $^{13}C\{^1H\}$ NMR ($CDCl_3$, 100 MHz): δ 12.0, 19.7, 20.2, 50.5, 55.7, 106.2, 115.9, 120.4 (x 2C), 123.5, 123.8, 123.9, 124.8, 126.7, 127.1, 128.0, 128.5, 129.1, 129.3, 135.6, 137.6, 137.7, 140.3, 150.0, 151.8. HRMS (ESI) m/z: $[M + H]^+$ calcd for $C_{27}H_{28}NO_2$ 398.2115, found 398.2109.

*2-(2-(Dimethylamino)naphthalen-1-yl)-6-methoxy-4-methylphenol (**20**).* 2-Methoxy-4-methylphenol (48 μL, 0.375 mmol) and *N*,*N*-dimethyl-2-aminonaphthalene[9f] **2b** (42.8 mg, 0.25 mmol) were reacted according to the general procedure. In this reaction, addition of TFA (1.25 equiv) and *t*-BuOO*t*-Bu (1.5 equiv) was needed to ensure full consumption of the 2-aminonaphthalene. Then, the reaction was quenched by the addition of CH_2Cl_2 and sat. $NaHCO_3$. The organic phase was separated, dried over $MgSO_4$, and evaporated under reduced pressure. The crude residue was purified by column chromatography (hexane/ethyl acetate 90:10) to afford compound **20** (75.1 mg, 98% yield) as a pale brown solid. ^1H NMR ($CDCl_3$, 400 MHz): δ 2.37 (s, 3H), 2.72 (s, 6H), 3.96 (s, 3H), 6.73−6.83 (m, 2H), 7.32−7.40 (m, 2H), 7.44 (d, 1H, J = 8.9 Hz), 7.80 (dt, 2H, J = 5.6, 2.5 Hz), 7.86 (d, 1H, J = 8.8 Hz). $^{13}C\{^1H\}$ NMR ($CDCl_3$, 100 MHz): δ 21.4, 43.9, 56.1, 111.8, 117.8, 124.5, 125.4, 125.7, 126.2, 126.4, 127.9, 128.3, 128.9, 129.1, 131.0, 133.7, 142.1, 146.9, 149.8. HRMS (ESI) m/z: $[M + H]^+$ calcd for $C_{20}H_{22}NO_2$ 308.1645, found 308.1640.

*2-(2-(Benzylamino)naphthalen-1-yl)-6-methoxy-4-methylphenol (**21**).* 2-Methoxy-4-methylphenol (48 μL, 0.375 mmol) and *N*-benzyl-2-aminonaphthalene **2f** (58.3 mg, 0.25 mmol) were reacted according to the general procedure. The crude residue was purified by column chromatography (hexane/ethyl acetate 85:15) to afford compound **21** (50 mg, 54% yield) as a brown solid. ^1H NMR ($CDCl_3$, 400 MHz): δ 2.38 (s, 3H), 3.97 (s, 3H), 4.51 (s, 2H), 6.69 (d, 1H, J = 0.9 Hz), 6.83 (d, 1H, J = 1.8 Hz), 7.11 (d, 1H, J = 9.0 Hz), 7.19−7.28 (m, 2H), 7.29−7.36 (m, 6H), 7.73 (d, 1H, J = 8.0 Hz), 7.75 (d, 1H, J = 8.9 Hz). $^{13}C\{^1H\}$ NMR ($CDCl_3$, 100 MHz): δ 21.3, 48.0, 56.1, 111.9, 114.2, 122.0, 122.1, 124.0, 124.4, 126.5, 127.0 (x 3C), 127.5, 128.1, 128.7, 129.5, 130.3, 133.6, 139.9, 141.7, 143.4, 147.4. HRMS (ESI) m/z: $[M + H]^+$ calcd for $C_{25}H_{24}NO_2$ 370.1802, found 370.1803.

*2-(2-((4-Chlorobenzyl)amino)naphthalen-1-yl)-6-methoxy-4-methylphenol (**22**).* 2-Methoxy-4-methylphenol (48 μL, 0.375 mmol) and *N*-(4-chlorobenzyl)-2-aminonaphthalene **2 g** (66.9 mg, 0.25 mmol) were reacted according to the general procedure. The crude residue was purified by column chromatography (hexane/ethyl acetate 85:15) to afford compound **22** (52.6 mg, 52% yield) as a pale brown solid. ^1H NMR ($CDCl_3$, 400 MHz): δ 2.36 (s, 3H), 3.97 (s, 3H), 4.45 (s, 2H), 6.64 (dd, 1H, J = 1.9, 0.8 Hz), 6.82 (d, 1H, J = 1.7 Hz), 7.01 (d, 1H, J = 9.0 Hz), 7.17−7.23 (m, 1H), 7.25 (s, 4H), 7.27−7.29 (m, 2H), 7.71 (d, 1H, J = 8.0 Hz), 7.72 (d, 1H, J = 9.0 Hz). $^{13}C\{^1H\}$ NMR ($CDCl_3$, 100 MHz): δ 21.3, 47.4, 56.1, 111.8, 114.0, 114.5, 121.9, 122.1, 124.1, 124.3, 126.6, 127.5, 128.2, 128.3, 128.8, 129.6, 130.4, 132.7, 133.6, 138.5, 141.6, 143.0, 147.4. HRMS (ESI) m/z: $[M + H]^+$ calcd for $C_{25}H_{23}ClNO_2$ 404.1412, found 404.1411. IR (KBr pellet): 3419 (s, broad), 2921 (s), 1506 (s), 1244 (m), 810 (s) cm^{-1}.

*2-Methoxy-6-(2-((4-methoxybenzyl)amino)naphthalen-1-yl)-4-methylphenol (**23**).* 2-Methoxy-4-methylphenol (48 μL, 0.375 mmol) and *N*-(4-methoxybenzyl)-2-aminonaphthalene **2l** (65.8 mg, 0.25 mmol) were reacted according to the general procedure. The crude residue was purified by column chromatography (hexane/ethyl acetate 85:15) to afford compound **23** (54.9 mg, 55% yield) as a brown solid. ^1H NMR ($CDCl_3$, 400 MHz): δ 2.38 (s, 3H), 3.80 (s, 3H), 3.99 (s, 3H), 4.45 (s, 2H), 6.67 (dd, 1H, J = 1.9, 0.8 Hz), 6.84 (d, 1H, J = 1.8 Hz), 6.85 (d, 1H, J = 2.1 Hz), 6.87 (d, 1H, J = 2.1 Hz), 7.13 (d, 1H, J = 9.0 Hz), 7.19−7.27 (m, 3H), 7.28−7.32 (m, 2H), 7.75 (t, 2H, J = 8.7 Hz). $^{13}C\{^1H\}$ NMR ($CDCl_3$, 100 MHz): δ 21.3, 47.5, 55.4, 56.1, 111.9, 114.0, 114.1, 114.3, 121.9, 122.1, 124.0, 124.4, 126.5, 127.4, 128.1, 128.2, 129.5, 130.3, 131.8, 133.6, 141.6, 143.5, 147.4, 158.7. HRMS (ESI) m/z: [M + H] + calcd for $C_{26}H_{26}NO_3$ 400.1907, found 400.1900.

*2-(2-(Heptylamino)naphthalen-1-yl)-6-methoxy-4-methylphenol (**24**).* 2-Methoxy-4-methylphenol (48 μL, 0.375 mmol) and *N*-heptyl-2-aminonaphthalene **2o** (60.3 mg, 0.25 mmol) were reacted according to the general procedure. The crude residue was purified by column chromatography (hexane/ethyl acetate 85:15) to afford compound **24** (66 mg, 70% yield) as a brown syrup. ^1H NMR ($CDCl_3$, 400 MHz): δ 0.91 (t, 3H, J = 6.9 Hz), 1.25−1.35 (m, 8H), 1.52−1.60 (m, 2H), 2.38 (s, 3H), 3.25 (t, 2H, J = 7.1 Hz), 3.99 (s, 3H), 6.66 (dd, 1H, J = 1.9, 0.8 Hz), 6.84 (d, 1H, J = 1.8 Hz), 7.18−7.24 (m, 2H), 7.27−7.33 (m, 2H), 7.76 (d, 1H, J = 8.1 Hz), 7.83 (d, 1H, J = 8.9 Hz). $^{13}C\{^1H\}$ NMR ($CDCl_3$, 100 MHz): δ 14.2, 21.3, 22.7, 27.0, 29.1, 29.8, 31.9, 44.4, 56.1, 111.8, 113.9, 114.2, 121.8, 122.2, 124.0, 124.4, 126.5, 127.3, 128.1, 129.5, 130.2, 133.6, 141.6, 143.9, 147.4. HRMS (ESI) m/z: $[M + H]^+$ calcd for $C_{25}H_{32}NO_2$ 378.2428, found 378.2421.

*2-(t-Butyl)-6-(2-((3-hydroxy-4-methoxybenzyl)amino)-naphthalen-1-yl)-4-methoxyphenol (**25**).* 2-*t*-Butyl-4-methoxyphenol (67.6 mg, 0.375 mmol) and *N*-(3-hydroxy-4-methoxybenzyl)-2-aminonaphthalene **2h** (69.8 mg, 0.25 mmol) were reacted according to the general procedure. The crude residue was purified by column chromatography (hexane/ethyl acetate 85:15) to afford compound **25** (105.2 mg, 92% yield) as a pale brown solid. ^1H NMR ($CDCl_3$, 400 MHz): δ 1.47 (s, 9H), 3.77 (s, 3H), 3.84 (s, 3H), 4.34 (d, 1H, J = 15.4 Hz), 4.39 (d, 1H, J = 15.5 Hz), 6.63 (d, 1H, J = 3.1 Hz), 6.73−6.80 (m, 2H), 6.87 (d, 1H, J = 1.6 Hz), 7.02 (d, 1H, J = 3.1 Hz), 7.14 (d, 1H, J = 9.0 Hz), 7.23 (ddd, 1H, J = 8.0, 6.4, 1.6 Hz), 7.26−7.35 (m, 2H), 7.74 (d, 1H, J = 8.0 Hz), 7.78 (d, 1H, J = 8.9 Hz). $^{13}C\{^1H\}$ NMR ($CDCl_3$, 100 MHz): δ 29.6, 35.3, 47.6, 55.8, 56.1, 110.8, 112.3 (x 2C), 113.5, 114.3, 114.9, 118.5, 122.3, 122.4, 123.7, 127.1, 127.6, 128.2, 130.4, 132.7, 133.9, 138.5, 144.2, 145.8, 145.9, 146.7, 153.4. HRMS (ESI) m/z: $[M + H]^+$ calcd for $C_{29}H_{32}NO_4$ 458.2326, found 458.2311.

*2-(2-(Butylamino)naphthalen-1-yl)-4,5-dimethoxyphenol (**26**).* 3,4-Dimethoxyphenol (57.8 mg, 0.375 mmol) and *N*-butyl-2-aminonaphthalene **2d** (49.8 mg, 0.25 mmol) were reacted according to the general procedure. The crude residue was purified by column chromatography (hexane/ethyl acetate 80:20) to afford compound **26** (60 mg, 68% yield) as a brown syrup. ^1H NMR ($CDCl_3$, 400 MHz): δ 0.91 (t, 3H, J = 7.3 Hz), 1.34 (sex, 2H, J = 7.5 Hz), 1.48−1.58 (m, 2H), 3.22 (t, 2H, J = 7.1 Hz), 3.81 (s, 3H), 3.96 (s, 3H), 6.70 (s, 1H), 6.75 (s, 1H), 7.17 (d, 1H, J = 9.0 Hz), 7.22 (ddd, 1H, J = 8.0, 6.0, 2.0 Hz), 7.27−7.35 (m, 2H), 7.74 (d, 1H, J = 8.1 Hz), 7.82 (d, 1H, J = 8.9 Hz). $^{13}C\{^1H\}$ NMR ($CDCl_3$, 100 MHz): δ 14.0, 20.2, 31.9, 43.9, 56.1, 56.5, 100.7, 111.6, 112.0, 114.0, 114.2, 122.2, 123.6, 127.1, 127.4, 128.3, 130.3, 134.1, 143.7, 144.7, 148.3, 150.2. HRMS (ESI) m/z: $[M + H]^+$ calcd for $C_{22}H_{26}NO_3$ 352.1907, found 352.1909.

*4-(2-((4-(t-Butyl)benzyl)amino)naphthalen-1-yl)-2-methoxy-6-methylphenol (**27**).* 2-Methoxy-6-methylphenol (51.8 mg, 0.375 mmol) and *N*-(4-*t*-butylbenzyl)-2-aminonaphthalene **2m** (72.4 mg, 0.25 mmol) were reacted according to the general procedure. The crude residue was purified by column chromatography (hexane/ethyl acetate 92:8) to afford compound **27** (75.5 mg, 71% yield) as a pale brown solid. ^1H NMR ($CDCl_3$, 400 MHz): δ 1.34 (s, 9H), 2.36 (s, 3H), 3.86 (s, 3H), 4.45 (s, 2H), 5.84 (bs, 1H), 6.72 (d, 1H, J = 1.3 Hz), 6.76 (d, 1H, J = 0.5 Hz), 7.18 (d, 1H, J = 9.0 Hz), 7.20−7.25 (m, 3H), 7.26−7.32 (m, 1H), 7.35 (d, 3H, J = 8.4 Hz), 7.74 (d, 1H, J = 8.0 Hz), 7.75 (d, 1H, J = 8.9 Hz). $^{13}C\{^1H\}$ NMR ($CDCl_3$, 100 MHz): δ 15.7, 31.5, 34.6, 48.1, 56.2, 111.0, 114.1, 120.4, 121.8, 124.4, 124.8, 125.6, 125.8, 126.2, 126.9, 127.3, 127.7, 128.0, 128.7, 134.0, 136.9, 143.1, 143.2, 147.0, 150.0. HRMS (ESI) m/z: $[M + H]^+$ calcd for $C_{29}H_{32}NO_2$ 426.2428, found 426.2420.

*(E)-2-(2-(Cinnamylamino)naphthalen-1-yl)-4,6-dimethylphenol (**28**).* 2,4-Dimethylphenol (45 μL, 0.375 mmol) and *N*-cinnamyl-2-

https://dx.doi.org/10.1021/acs.joc.0c00874
J. Org. Chem. 2021, 86, 79−90

aminonaphthalene **2k** (64.8 mg, 0.25 mmol) were reacted according to the general procedure. The crude residue was purified by column chromatography (hexane/ethyl acetate 97:3) to afford compound **28** (53.9 mg, 57% yield) as a yellow solid. ^{1}H NMR ($CDCl_3$, 400 MHz): δ 2.31 (s, 3H), 2.33 (s, 3H), 4.05 (dd, 2H, J = 5.4, 1.6 Hz), 6.25 (dt, 1H, J = 15.9, 5.4 Hz), 6.54 (d, 1H, J = 15.9 Hz), 6.85−6.89 (m, 1H), 7.07 (dd, 1H, J = 1.4, 0.6 Hz), 7.17−7.36 (m, 9H), 7.74 (d, 1H, J = 8.4 Hz), 7.82 (d, 1H, J = 8.9 Hz). ^{13}C{^{1}H} NMR ($CDCl_3$, 100 MHz): δ 16.4, 20.7, 46.0, 112.5, 114.2, 121.1, 122.3, 123.8, 125.0, 126.4, 127.1, 127.3, 127.6 (x 2C), 128.2, 128.7, 129.7, 130.1, 130.2, 131.2, 132.1, 133.9, 136.8, 144.2, 150.0. HRMS (ESI) m/z: $[M + H]^+$ calcd for $C_{27}H_{26}NO$ 380.2009, found 380.2001.

*4-(2-((Furan-2-ylmethyl)amino)naphthalen-1-yl)-2,5-dimethylphenol (**29**).* 2,5-Dimethylphenol (45.8 mg, 0.375 mmol) and *N*-(2-furylmethyl)-2-aminonaphthalene **2p** (55.8 mg, 0.25 mmol) were reacted according to the general procedure. The crude residue was purified by column chromatography (hexane/ethyl acetate 90:10) to afford compound **29** (33 mg, 38% yield) as a brown solid. ^{1}H NMR ($CDCl_3$, 400 MHz): δ 1.85 (s, 3H), 2.25 (s, 3H), 4.41 (s, 2H), 6.11 (dd, 1H, J = 3.2, 0.8 Hz), 6.26 (dd, 1H, J = 3.2, 1.9 Hz), 6.81 (s, 1H), 6.88 (s, 1H), 7.08−7.14 (m, 1H), 7.18−7.32 (m, 4H), 7.72−7.75 (m, 1H), 7.77 (d, 1H, J = 8.8 Hz). ^{13}C{^{1}H} NMR ($CDCl_3$, 100 MHz): δ 15.5, 19.1, 41.9, 106.8, 110.4, 114.5, 117.1, 120.2, 122.1 (x 2C), 124.3, 126.3, 127.7, 127.8, 128.0, 128.5, 133.8 (x 2C), 137.4, 141.8, 142.5, 153.4, 153.6. HRMS (ESI) m/z: $[M + H]^+$ calcd for $C_{23}H_{22}NO_2$ 344.1645, found 344.1646.

*4-(2-(Benzylamino)naphthalen-1-yl)-2,6-dimethylphenol (**30**).* 2,6-Dimethylphenol **1b** (45.8 mg, 0.375 mmol) and *N*-benzyl-2-aminonaphthalene **2f** (58.3 mg, 0.25 mmol) were reacted according to the general procedure. The crude residue was purified by column chromatography (hexane/ethyl acetate 90:10) to afford compound **30** (66.9 mg, 76% yield) as an orange syrup. The reaction was also performed on a 2 mmol scale, affording compound **30** (523 mg, 74% yield). ^{1}H NMR ($CDCl_3$, 400 MHz): δ 2.29 (s, 6H), 4.43 (s, 2H), 6.92−6.94 (m, 2H), 7.08 (d, 1H, J = 8.9 Hz), 7.16 (ddd, 1H, J = 8.0, 6.5, 1.5 Hz), 7.20−7.32 (m, 7H), 7.67 (dd, 1H, J = 1.9, 1.1 Hz), 7.69 (s, 1H). ^{13}C{^{1}H}NMR ($CDCl_3$, 100 MHz): δ 16.1, 48.5, 114.4, 120.4, 121.8, 124.1, 124.5, 126.1, 127.1 (x 2C), 127.4, 127.9, 128.5, 128.6, 128.7, 131.3, 134.1, 140.0, 143.0, 151.8. HRMS (ESI) m/z: $[M + H]^+$ calcd for $C_{25}H_{24}NO$ 354.1852, found 354.1848. IR (KBr pellet): 3419 (s, broad), 2924 (m), 1200 (s), 746 (m) cm^{-1}.

■ ASSOCIATED CONTENT

Supporting Information

The Supporting Information is available free of charge at https://pubs.acs.org/doi/10.1021/acs.joc.0c00874.

Kinetic data and mechanistic studies as well as full spectroscopic data for all compounds (PDF)

X-ray diffraction analysis results of compound 20 (CIF)

■ AUTHOR INFORMATION

Corresponding Author

Doron Pappo − *Department of Chemistry, Ben-Gurion University of the Negev, Beer-Sheva 84105, Israel;* orcid.org/0000-0002-8363-8709; Email: pappod@bgu.ac.il

Authors

Vlada Vershinin − *Department of Chemistry, Ben-Gurion University of the Negev, Beer-Sheva 84105, Israel*

Hagit Forkosh − *Department of Chemistry, Ben-Gurion University of the Negev, Beer-Sheva 84105, Israel*

Mor Ben-Lulu − *Department of Chemistry, Ben-Gurion University of the Negev, Beer-Sheva 84105, Israel*

Anna Libman − *Department of Chemistry, Ben-Gurion University of the Negev, Beer-Sheva 84105, Israel*

Complete contact information is available at: https://pubs.acs.org/10.1021/acs.joc.0c00874

Author Contributions

‡V.V. and H.F. contributed equally.

Notes

The authors declare no competing financial interest.

■ ACKNOWLEDGMENTS

The authors would like to thank the COST-CHAOS organization for funding the participation of HF and DP in their conferences. This work was supported by the Israel Science Foundation (grant number 655/20).

■ REFERENCES

(1) (a) Shalit, H.; Dyadyuk, A.; Pappo, D. Selective Oxidative Phenol Coupling by Iron Catalysis. *J. Org. Chem.* **2019**, *84*, 1677−1686. (b) Kozlowski, M. C. Oxidative Coupling in Complexity Building Transforms. *Acc. Chem. Res.* **2017**, *50*, 638−643. (c) Yang, X.-H.; Song, R.-J.; Xie, Y.-X.; Li, J.-H. Iron Catalyzed Oxidative Coupling, Addition, and Functionalization. *ChemCatChem* **2016**, *8*, 2429−2445. (d) Jia, F.; Li, Z. Iron-catalyzed/mediated oxidative transformation of C−H bonds. *Org. Chem. Front.* **2014**, *1*, 194−214.

(2) (a) Narute, S.; Pappo, D. Iron Phosphate Catalyzed Asymmetric Cross-Dehydrogenative Coupling of 2-Naphthols with β-Ketoesters. *Org. Lett.* **2017**, *19*, 2917−2920. (b) Gaster, E.; Vainer, Y.; Regev, A.; Narute, S.; Sudheendran, K.; Werbeloff, A.; Shalit, H.; Pappo, D. Significant Enhancement in the Efficiency and Selectivity of Iron-Catalyzed Oxidative Cross-Coupling of Phenols by Fluoroalcohols. *Angew. Chem., Int. Ed.* **2015**, *54*, 4198−4202. (c) Kshirsagar, U. A.; Parnes, R.; Goldshtein, H.; Ofir, R.; Zarivach, R.; Pappo, D. Aerobic Iron-Based Cross-Dehydrogenative Coupling Enables Efficient Diversity-Oriented Synthesis of Coumestrol-Based Selective Estrogen Receptor Modulators. *Chem. − Eur. J.* **2013**, *19*, 13575−13583. (d) Parnes, R.; Kshirsagar, U. A.; Werbeloff, A.; Regev, C.; Pappo, D. Ligand-Controlled Iron-Catalyzed Coupling of α-Substituted β-Ketoesters with Phenols. *Org. Lett.* **2012**, *14*, 3324−3327. (e) Guo, X.; Yu, R.; Li, H.; Li, Z. Iron-Catalyzed Tandem Oxidative Coupling and Annulation: An Efficient Approach to Construct Polysubstituted Benzofurans. *J. Am. Chem. Soc.* **2009**, *131*, 17387−17393.

(3) Kshirsagar, U. A.; Regev, C.; Parnes, R.; Pappo, D. Iron-Catalyzed Oxidative Cross-Coupling of Phenols and Alkenes. *Org. Lett.* **2013**, *15*, 3174−3177.

(4) (a) Vershinin, V.; Dyadyuk, A.; Pappo, D. Iron-catalyzed selective oxidative arylation of phenols and biphenols. *Tetrahedron* **2017**, *73*, 3660−3668. (b) Dyadyuk, A.; Sudheendran, K.; Vainer, Y.; Vershinin, V.; Shames, A. I.; Pappo, D. Direct Synthesis of Polyaryls by Consecutive Oxidative Cross-Coupling of Phenols with Arenes. *Org. Lett.* **2016**, *18*, 4324−4327.

(5) (a) Shalit, H.; Libman, A.; Pappo, D. meso-Tetraphenylporphyrin Iron Chloride Catalyzed Selective Oxidative Cross-Coupling of Phenols. *J. Am. Chem. Soc.* **2017**, *139*, 13404−13413. (b) Libman, A.; Shalit, H.; Vainer, Y.; Narute, S.; Kozuch, S.; Pappo, D. Synthetic and Predictive Approach to Unsymmetrical Biphenols by Iron-Catalyzed Chelated Radical-Anion Oxidative Coupling. *J. Am. Chem. Soc.* **2015**, *137*, 11453−11460. (c) Narute, S.; Parnes, R.; Toste, F. D.; Pappo, D. Enantioselective Oxidative Homocoupling and Cross-Coupling of 2-Naphthols Catalyzed by Chiral Iron Phosphate Complexes. *J. Am. Chem. Soc.* **2016**, *138*, 16553−16560.

(6) (a) Ben-Lulu, M.; Gaster, E.; Libman, A.; Pappo, D. Synthesis of Biaryl-Bridged Cyclic Peptides via Catalytic Oxidative Cross-Coupling Reactions. *Angew. Chem., Int. Ed.* **2020**, *59*, 4835−4839. (b) Grzybowski, M.; Sadowski, B.; Butenschön, H.; Gryko, D. T. Synthetic Applications of Oxidative Aromatic Coupling—From Biphenols to Nanographenes. *Angew. Chem., Int. Ed.* **2019**, *59*, 2−3027.

(7) (a) Ding, K.; Li, X.; Ji, B.; Guo, H.; Kitamura, M. Ten years of research on NOBIN chemistry. *Curr. Org. Synth.* **2005**, *2*, 499−545.

(b) Kočovský, P.; Vyskočil, Š.; Smrčina, M. Non-Symmetrically Substituted 1,1'-Binaphthyls in Enantioselective Catalysis. *Chem. Rev.* **2003**, *103*, 3213−3246. (c) Vyskocil, S.; Jaracz, S.; Smrcina, M.; Sticha, M.; Hanus, V.; Polasek, M.; Kocovsky, P. Synthesis of N-alkylated and N-arylated derivatives of 2-amino-2′-hydroxy-1,1′-binaphthyl (NOBIN) and 2,2′-diamino-1,1′-binaphthyl and their application in the enantioselective addition of diethylzinc to aromatic aldehydes. *J. Org. Chem.* **1998**, *63*, 7727−7737.

(8) (a) Pavitt, A. S.; Bylaska, E. J.; Tratnyek, P. G. Oxidation potentials of phenols and anilines: correlation analysis of electrochemical and theoretical values. *Enviorn. Sci-Proc. Imp.* **2017**, *19*, 339−349. (b) Erickson, P. R.; Walpen, N.; Guerard, J. J.; Eustis, S. N.; Arey, J. S.; McNeill, K. Controlling Factors in the Rates of Oxidation of Anilines and Phenols by Triplet Methylene Blue in Aqueous Solution. *J. Phys. Chem. A* **2015**, *119*, 3233−3243. (c) Suatoni, J. C.; Snyder, R. E.; Clark, R. O. Voltammetric studies of phenol and aniline ring substitution. *Anal. Chem.* **1961**, *33*, 1894−1897.

(9) (a) Paniak, T. J.; Kozlowski, M. C. Aerobic Catalyzed Oxidative Cross-Coupling of N,N-Disubstituted Anilines and Aminonaphthalenes with Phenols and Naphthols. *Org. Lett.* **2020**, *22*, 1765−1770. (b) Purtsas, A.; Kataeva, O.; Knolker, H. J. Iron-Catalyzed Oxidative C-C Cross-Coupling Reaction of Tertiary Anilines with Hydroxyarenes by Using Air as Sole Oxidant. *Chem. − Eur. J.* **2019**, *25*, 13759−13765. (c) Bering, L.; D'Ottavio, L.; Sirvinskaite, G.; Antonchick, A. P. Nitrosonium ion catalysis: aerobic, metal-free cross-dehydrogenative carbon−heteroatom bond formation. *Chem. Commun.* **2018**, *54*, 13022−13025. (d) Schulz, L.; Enders, M.; Elsler, B.; Schollmeyer, D.; Dyballa, K. M.; Franke, R.; Waldvogel, S. R. Reagent- and Metal-Free Anodic C−C Cross-Coupling of Aniline Derivatives. *Angew. Chem., Int. Ed.* **2017**, *56*, 4877−4881. (e) Fritsche, R. F.; Theumer, G.; Kataeva, O.; Knölker, H.-J. Iron-Catalyzed Oxidative C−C and N−N Coupling of Diarylamines and Synthesis of Spiroacridines. *Angew. Chem., Int. Ed.* **2017**, *56*, 549−553. (f) Matsumoto, K.; Yoshida, M.; Shindo, M. Heterogeneous Rhodium-Catalyzed Aerobic Oxidative Dehydrogenative Cross-Coupling: Nonsymmetrical Biaryl Amines. *Angew. Chem., Int. Ed.* **2016**, *55*, 5272−5276. (g) Berkessa, S. C.; Clarke, Z. J. F.; Fotie, J.; Bohle, D. S.; Grimm, C. C. Silver(I)-mediated regioselective oxidative cross-coupling of phenol and aniline derivatives resulting in 2′-aminobiphenyl-2-ols. *Tetrahedron Lett.* **2016**, *57*, 1613−1618. (h) Jin, R.; Patureau, F. W. Mild, Periodate-Mediated, Dehydrogenative C−N Bond Formation with Phenothiazines and Phenols. *Org. Lett.* **2016**, *18*, 4491−4493. (i) Chandrasekharam, M.; Chiranjeevi, B.; Gupta, K. S. V.; Sridhar, B. Iron-Catalyzed Regioselective Direct Oxidative Aryl−Aryl Cross-Coupling. *J. Org. Chem.* **2011**, *76*, 10229−10235. (j) Yusa, Y.; Kaito, I.; Akiyama, K.; Mikami, K. Asymmetric catalysis of homo-coupling of 3-substituted naphthylamine and hetero-coupling with 3-substituted naphthol leading to 3,3′-dimethyl-2,2′-diaminobinaphthyl and −2-amino-2′-hydroxybinaphthyl. *Chirality* **2010**, *22*, 224−228. (k) Smrcina, M.; Vyskocil, S.; Maca, B.; Polasek, M.; Claxton, T. A.; Abbott, A. P.; Kocovsky, P. Selective Cross-Coupling of 2-Naphthol and 2-Naphthylamine Derivatives. A Facile Synthesis of 2,2′,3-Trisubstituted and 2,2′,3,3′-Tetrasubstituted 1,1'-Binaphthyls. *J. Org. Chem.* **1994**, *59*, 2156−2163. (l) Smrcina, M.; Lorenc, M.; Hanus, V.; Sedmera, P.; Kocovsky, P. Synthesis of enantiomerically pure 2,2′-dihydroxy-1,1′-binaphthyl, 2,2′-diamino-1,1′-binaphthyl, and 2-amino-2′-hydroxy-1,1′-binaphthyl. Comparison of processes operating as diastereoselective crystallization and as second order asymmetric transformation. *J. Org. Chem.* **1992**, *57*, 1917−1920. (m) Vyskocil, S.; Smrcina, M.; Lorenc, M.; Kocovsky, P.; Vyskocil, S.; Lorenc, M.; Hanus, V.; Polasek, M. On the 'Novel two-phase oxidative cross-coupling of the two-component molecular crystal of 2-naphthol and 2-naphthylamine. *Chem. Commun.* **1998**, 585−586. (n) Smrčina, M.; Lorenc, M.; Hanuš, V.; Kočovský, P. A Facile Synthesis of 2-Amino-2′-hydroxy-1,1′-binaphthyl and 2,2′-Diamino-1,1′-binaphthyl by Oxidative Coupling Using Copper(II) Chloride. *Synlett* **1991**, *1991*, 231−232.

(10) Matsumoto, K.; Dougomori, K.; Tachikawa, S.; Ishii, T.; Shindo, M. Aerobic Oxidative Homocoupling of Aryl Amines Using Heterogeneous Rhodium Catalysts. *Org. Lett.* **2014**, *16*, 4754−4757.

(11) Vershinin, V.; Pappo, D. M[TPP]Cl (M = Fe or Mn)-Catalyzed Oxidative Amination of Phenols by Primary and Secondary Anilines. *Org. Lett.* **2020**, *22*, 1941−1946.

(12) Forkosh, H.; Vershinin, V.; Reiss, H.; Pappo, D. Stereoselective Synthesis of Optically Pure 2-Amino-2′-hydroxy-1,1′-binaphthyls. *Org. Lett.* **2018**, *20*, 2459−2463.

(13) (a) Egami, H.; Matsumoto, K.; Oguma, T.; Kunisu, T.; Katsuki, T. Enantioenriched Synthesis of C1-Symmetric BINOLs: Iron-Catalyzed Cross-Coupling of 2-Naphthols and Some Mechanistic Insight. *J. Am. Chem. Soc.* **2010**, *132*, 13633−13635. (b) Egami, H.; Katsuki, T. Iron-Catalyzed Asymmetric Aerobic Oxidation: Oxidative Coupling of 2-Naphthols. *J. Am. Chem. Soc.* **2009**, *131*, 6082−6083.

(14) Regev, A.; Shalit, H.; Pappo, D. Iron-Catalyzed Oxidative C−C and C−O Coupling of Halophenols to α-Substituted β-Keto Esters. *Synthesis* **2015**, *47*, 1716−1725.

(15) Burés, J. A Simple Graphical Method to Determine the Order in Catalyst. *Angew. Chem., Int. Ed.* **2016**, *55*, 2028−2031.

(16) (a) Cleland, W. The kinetics of enzyme-catalyzed reactions with two or more substrates or products: III Prediction of initial velocity and inhibition patterns by inspection. *Biochim. Biophys. Acta.* **1963**, *67*, 188−196. (b) Cleland, W. W. The kinetics of enzyme-catalyzed reactions with two or more substrates or products: I Nomenclature and rate equations. *Biochim. Biophys. Acta.* **1963**, *67*, 104−137. (c) Cleland, W. The kinetics of enzyme-catalyzed reactions with two or more substrates or products: II Inhibition: Nomenclature and theory. *Biochim. Biophys. Acta.* **1963**, *67*, 173−187.

(17) Cook, P. F.; Cleland, W. W. Enzyme kinetics and mechanism. *Science* **2007**, *17*, 380−381.

(18) Punekar, N. S., *Enzymes*. Springer: 2018; 221−230.

(19) Frieden, C. The Calculation of an Enzyme-Substrate Dissociation Constant from the Over-all Initial Velocity for Reactions Involving Two Substrates. *J. Am. Chem. Soc.* **1957**, *79*, 1894−1896.

(20) (a) Purich, D. L., *Enzyme kinetics: catalysis and control: a reference of theory and best-practice methods*. Elsevier: 2010; (b) Bisswanger, H., *Enzyme kinetics: principles and methods*. John Wiley & Sons: 2017.

(21) (a) Blackmond, D. G. Kinetic Profiling of Catalytic Organic Reactions as a Mechanistic Tool. *J. Am. Chem. Soc.* **2015**, *137*, 10852−10866. (b) Blackmond, D. G. Reaction Progress Kinetic Analysis: A Powerful Methodology for Mechanistic Studies of Complex Catalytic Reactions. *Angew. Chem., Int. Ed.* **2005**, *44*, 4302−4320.

(22) Iranpoor, N.; Adibi, H. Iron(III) Trifluoroacetate as an Efficient Catalyst for Solvolytic and Nonsolvolytic Nucleophilic Ring Opening of Epoxides. *Bull. Chem. Soc. Japan* **2000**, *73*, 675−680.

(23) Abdel-Magid, A. F.; Carson, K. G.; Harris, B. D.; Maryanoff, C. A.; Shah, R. D. Reductive Amination of Aldehydes and Ketones with Sodium Triacetoxyborohydride. Studies on Direct and Indirect Reductive Amination Procedures. *J. Org. Chem.* **1996**, *61*, 3849−3862.

https://dx.doi.org/10.1021/acs.joc.0c00874
J. Org. Chem. 2021, 86, 79−90